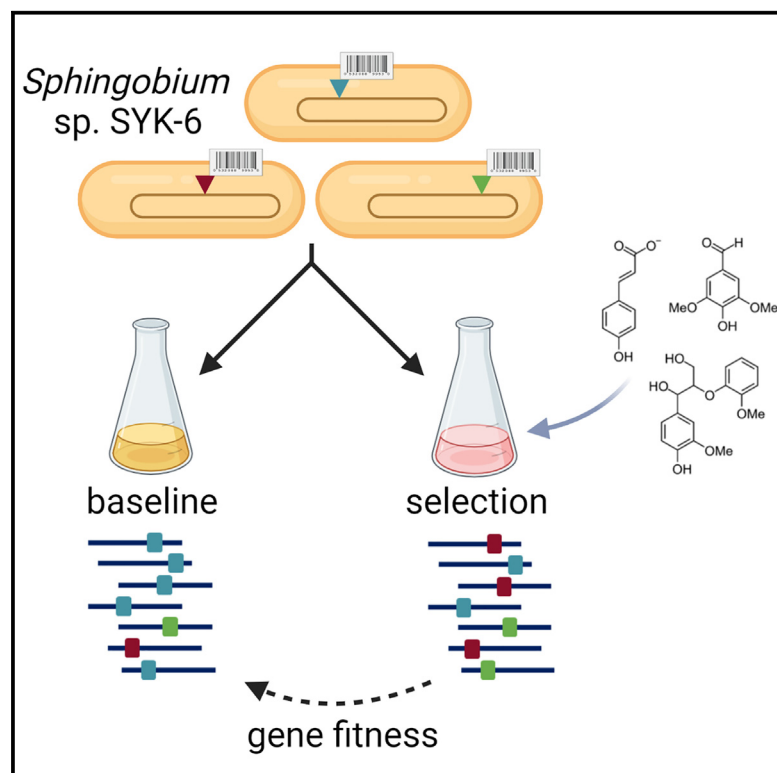


# Multiplexed fitness profiling by RB-TnSeq elucidates pathways for lignin-related aromatic catabolism in *Sphingobium* sp. SYK-6

## Graphical abstract



## Authors

Alissa Bleem, Ryo Kato, Zoe A. Kellermyer, ..., Naofumi Kamimura, Eiji Masai, Gregg T. Beckham

## Correspondence

emasai@vos.nagaokaut.ac.jp (E.M.), gregg.beckham@nrel.gov (G.T.B.)

## In brief

Bleem et al. develop a randomly barcoded transposon insertion (RB-TnSeq) library in *Sphingobium* sp. SYK-6 and then apply it to quantify gene fitness in aromatic catabolism and stress tolerance conditions. The library identifies details of SYK-6 metabolism, provides metabolic engineering targets for biological lignin valorization, and enables future fitness profiling.

## Highlights

- An RB-TnSeq library is generated in the aromatic catabolic bacterium, *Sphingobium* sp. SYK-6
- The library is enriched under dozens of growth conditions to determine gene fitness
- Fitness profiling identifies details of lignin-related aromatic catabolism and tolerance
- This RB-TnSeq library is a resource for future fitness profiling in additional conditions



## Resource

# Multiplexed fitness profiling by RB-TnSeq elucidates pathways for lignin-related aromatic catabolism in *Sphingobium* sp. SYK-6

Alissa Bleem,<sup>1</sup> Ryo Kato,<sup>2</sup> Zoe A. Kellermeyer,<sup>1</sup> Rui Katahira,<sup>1</sup> Masahiro Miyamoto,<sup>2</sup> Koh Niinuma,<sup>2</sup> Naofumi Kamimura,<sup>2</sup> Eiji Masai,<sup>2,\*</sup> and Gregg T. Beckham<sup>1,3,\*</sup>

<sup>1</sup>Renewable Resources and Enabling Sciences Center, National Renewable Energy Laboratory, Golden, CO 80401, USA

<sup>2</sup>Department of Materials Science and Bioengineering, Nagaoka University of Technology, Nagaoka, Niigata 940-2188, Japan

<sup>3</sup>Lead contact

\*Correspondence: [emasai@vos.nagaokaut.ac.jp](mailto:emasai@vos.nagaokaut.ac.jp) (E.M.), [gregg.beckham@nrel.gov](mailto:gregg.beckham@nrel.gov) (G.T.B.)

<https://doi.org/10.1016/j.celrep.2023.112847>

## SUMMARY

Bioconversion of lignin-related aromatic compounds relies on robust catabolic pathways in microbes. *Sphingobium* sp. SYK-6 (SYK-6) is a well-characterized aromatic catabolic organism that has served as a model for microbial lignin conversion, and its utility as a biocatalyst could potentially be further improved by genome-wide metabolic analyses. To this end, we generate a randomly barcoded transposon insertion mutant (RB-TnSeq) library to study gene function in SYK-6. The library is enriched under dozens of enrichment conditions to quantify gene fitness. Several known aromatic catabolic pathways are confirmed, and RB-TnSeq affords additional detail on the genome-wide effects of each enrichment condition. Selected genes are further examined in SYK-6 or *Pseudomonas putida* KT2440, leading to the identification of new gene functions. The findings from this study further elucidate the metabolism of SYK-6, while also providing targets for future metabolic engineering in this organism or other hosts for the biological valorization of lignin.

## INTRODUCTION

Lignin is a complex aromatic polymer that serves as a structural material in plant cell walls and is typically a waste product in lignocellulosic biorefineries,<sup>1,2</sup> and the chemical heterogeneity of lignin has long hindered its valorization to single products.<sup>3–6</sup> Fortunately, some microbes have evolved metabolic pathways for “biological funneling” of diverse lignin-related aromatics toward central metabolism,<sup>7–15</sup> including for the production of a single, value-added product through metabolic engineering.<sup>16–21</sup> The use of biological funneling for lignin valorization requires robust strain development, including overcoming bottlenecks, increasing metabolic flux, improving feedstock tolerance, and incorporating new pathways for assimilation of aromatic compounds.<sup>22</sup> This in turn demands thorough genomic characterization of aromatic catabolism under a variety of relevant conditions.

Over the past few decades, *Sphingobium* sp. SYK-6 (hereafter, SYK-6) has become one of the most prominent model systems for the conversion of lignin-related aromatic compounds with rich diversity in its native catabolic pathways.<sup>11,23,24</sup> Isolated from a wastewater treatment pond for kraft pulping, this gram-negative bacterium was originally characterized for its ability to cleave the biphenyl 5,5'-dehydrodivanillate (DDVA)<sup>25</sup> and subsequently convert the resulting aromatic monomers via the protococatechuate 4,5-cleavage pathway.<sup>26</sup> Dozens of gene functions have since been described,<sup>11,23,27</sup> and heterologous

expression of SYK-6 pathways has enabled conversion of lignin-related aromatic compounds toward value-added products in *Pseudomonas putida*.<sup>28–32</sup> The desire to leverage the lignin-degrading capabilities of SYK-6 for biological funneling has prompted many pathway-specific studies of its aromatic catabolism, wherein each enzymatic step for assimilation and conversion of a lignin-related compound is genetically identified and/or biochemically characterized to demonstrate function.<sup>11,23,33–37</sup> This approach is fruitful for reaction characterization, but opportunities remain for consideration of redundant or global elements of aromatic catabolism, such as regulation, transport, and cofactor balancing, which could be essential to achieve industrially viable strain performance for the conversion of lignin-derived products in SYK-6 itself or in engineered strains that harbor its pathways.

Randomly barcoded transposon insertion sequencing (RB-TnSeq)<sup>38</sup> offers a high-throughput, genome-wide approach to examine the role of all nonessential genes during growth in a condition of interest, thereby illuminating a panel of influential genes for growth in that condition. The approach uses an initial TnSeq experiment to map the location of barcoded transposons within a host genome, and then it assigns a fitness value to each gene by enumerating PCR-amplified barcodes after and before a desired selection in a process termed BarSeq (Figure 1A). Gene fitness equates roughly to the log<sub>2</sub> ratio of barcodes after versus before selection, and greater fitness magnitudes correspond to greater importance of a gene for growth under the selection.



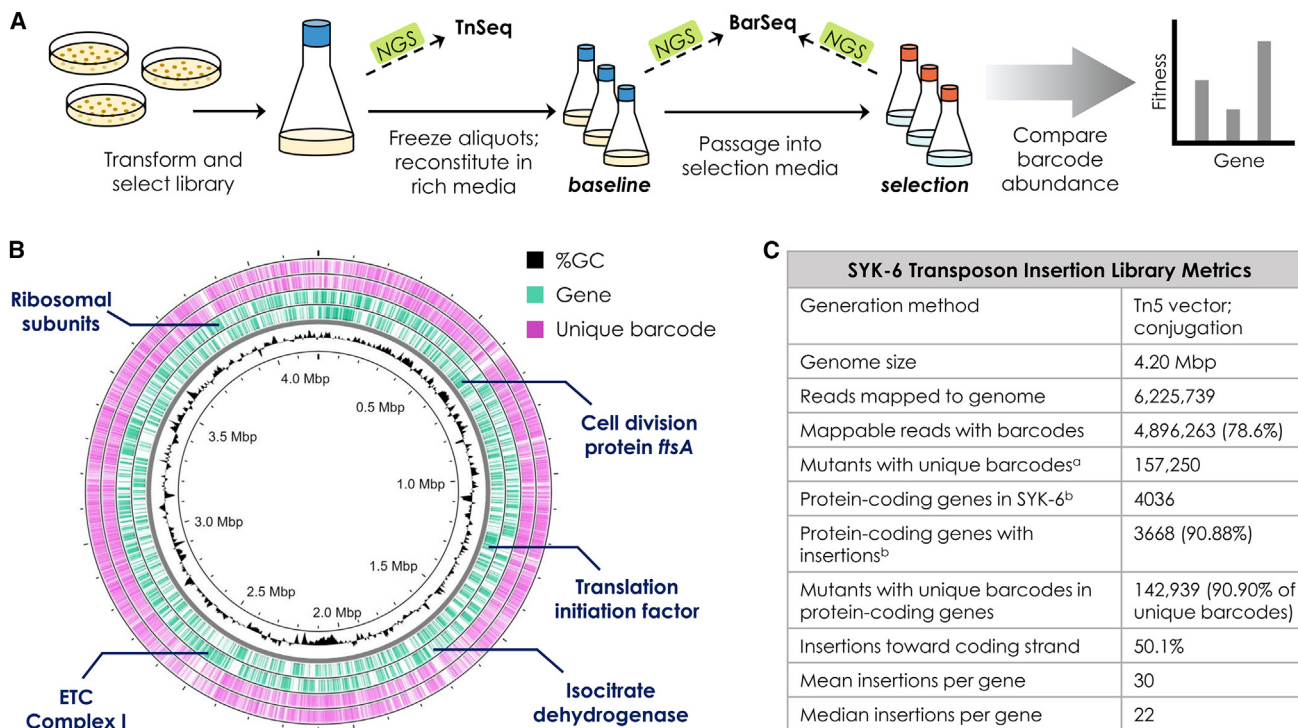


**Figure 1. Generation of an RB-TnSeq library in SYK-6**

(A) Workflow for library assembly and RB-TnSeq. Transconjugants were selected and cultivated, and then TnSeq mapped the location of each barcoded insertion to a specific locus in the genome. Subsequent BarSeq experiments compared the abundance of barcodes between a selection condition and a baseline condition to generate gene fitness scores.

(B) A map of the SYK-6 genome illustrating GC content (black, origin corresponds to 50% GC), protein-coding genes (teal), and Tn5-mediated insertion sites for 157,250 unique barcodes (magenta). The inner and outer rings of the gene and barcode tracks correspond to the sense (+) and antisense (−) strands, respectively. Regions of no transposon insertion, indicating essentiality, are labeled with their annotations. The genome map was generated with Proksee.<sup>47</sup>

(C) Quality metrics, obtained from TnSeq, for the RB-TnSeq library in SYK-6. <sup>a</sup>A unique barcode mapped to its primary location at least 10 times, at least 75% of its reads mapped to the primary location, and its second most frequent insertion location was at least eight times less frequent than the primary location. <sup>b</sup>Includes genes on the SYK-6 plasmid, pSLGP.

Each barcoded transposon experiment utilizes a unique sequence index on one of its PCR primers, enabling parallel mutant fitness profiling for dozens of conditions in a single Illumina sequencing run.<sup>38</sup> RB-TnSeq has been widely adopted for a variety of gene discovery applications, including those related to virulence,<sup>39</sup> stress,<sup>40</sup> catabolism,<sup>41–43</sup> and mutualism.<sup>44,45</sup> Experimental and analytical methods to improve the resolution of RB-TnSeq have also been described.<sup>46</sup>

In this study, we generated an RB-TnSeq library in SYK-6 and applied it for characterization of lignin-related aromatic catabolism. The library contains Tn5 transposon insertions in 91% of protein-coding genes, enabling deep characterization of gene fitness across the entire genome. Initial screens validated the importance of known catabolic pathways, and fitness profiling also identified previously unknown gene contributors. Selection conditions included growth on lignin-related aromatic monomers, growth on 5-5-,  $\beta$ -1-, and  $\beta$ -O-4-type dimers, and tolerance to acetic acid and methionine (L-Met) stress. Selected genes were further characterized by clean knockouts in SYK-6 or heterologous expression in *P. putida* KT2440 (hereafter, *P. putida*), which identified a previously unknown transporter (SLG\_02160) involved in the uptake of L-Met and a trehalose

biosynthesis cassette (*otsBA*) involved in tolerance to acetic acid. A critical role for several other known catabolic genes was also established, including degradation pathways for syringyl (S)-, guaiacyl (G)-, and *p*-hydroxyphenyl (H)-type lignin-related aromatic compounds. Overall, the establishment of an RB-TnSeq library in SYK-6 enables future fitness profiling in this bacterium under a wide variety of conditions.

## RESULTS

### Generation of a complex mutant library in SYK-6 using randomly barcoded transposons

A randomly barcoded transposon insertion library was constructed in SYK-6 using a previously described approach<sup>38</sup> with a Tn5 transposon insertion vector library (see STAR Methods). Transformants were pooled into selective medium and genomic DNA (gDNA) was prepared for TnSeq, wherein the genomic location of each transposon barcode was identified. Sequencing revealed dense coverage of the SYK-6 genome, with over 150,000 mutants containing a unique barcode mapping to its primary location at least 10 times (Figures 1B and 1C; Table S1). Insertions were observed in 3,668 of 4,036

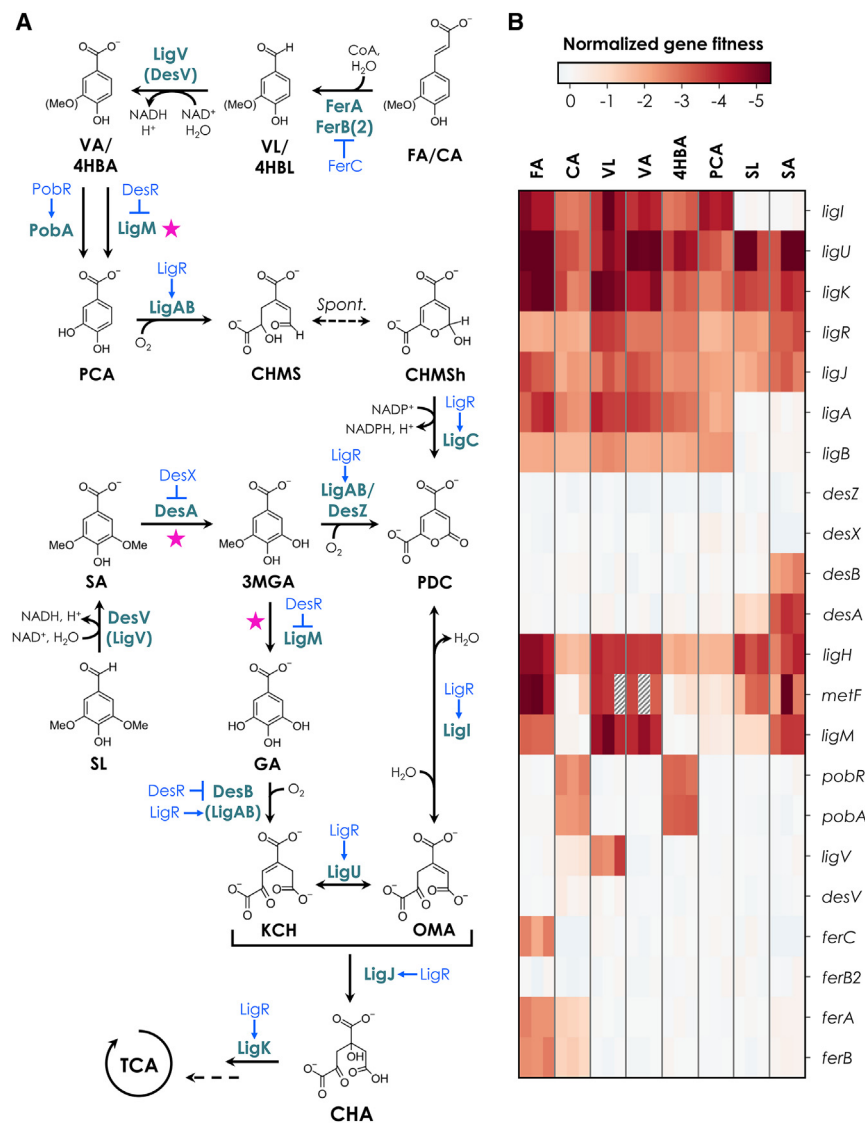


**Figure 2. Fitness profiling of aromatic catabolic pathways in SYK-6**

(A) Known pathways for aromatic catabolism<sup>11,23</sup> are pictured on the left. Each enzyme is shown in teal, transcriptional regulators are shown in blue (T shape for negative regulation; arrow for positive regulation) for the given catabolic genes, and pink stars indicate demethylation steps that rely on THF-mediated C1 metabolism. FA, ferulate; CA, *p*-coumarate; VL, vanillin; 4HBL, 4-hydroxybenzaldehyde; VA, vanillate; 4HBA, 4-hydroxybenzoate; PCA, protocatechuate; CHMS, 4-carboxy-2-hydroxy-6-semialdehyde; CHMSH, hemiacetal form of CHMS; PDC, 2-pyrone-4,6-dicarboxylate; SL, syringaldehyde; SA, syringate; 3MGA, 3-*O*-methylgallate; GA, gallate; OMA, 4-oxalomesaconate; KCH, 2-keto-4-carboxy-3-hexenedioate; CHA, 4-carboxy-4-hydroxy-2-oxoadipate.

(B) Normalized fitness values for genes in the metabolic map, each calculated from a biological replicate of the SYK-6 library relative to a rich medium (LB) baseline. Note that the *desR* and *ligC* genes lacked sufficient insertion counts to qualify for fitness analysis, so they are not included. Gray hashing indicates a gene that failed to qualify for analysis due to a lack of sufficient insertion counts in the enrichment replicate. Quantitative data for plots can be found in Table S5.

protein-coding genes (91%), with a mean of 30 unique barcodes per gene. The remaining 9% of genes without insertions provided an estimate of gene essentiality, and most of these were annotated with essential functions such as cell division, central metabolism, and translation (Figure 1B; Table S2). Interestingly, 19 of these prospective essential genes were located on the single SYK-6 plasmid, pSLGP, which likely originated from a related *Sphingobium* species.<sup>27</sup>

### Fitness profiling validates pathways for aromatic catabolism

To identify genes involved in catabolism of lignin-related aromatic compounds, three aliquots of the frozen SYK-6 transposon insertion library were thawed and grown to mid-log phase in rich medium. Cell pellets were withdrawn and gDNA was collected from these “time zero” baseline samples, and then a portion of each culture was passaged into minimal medium with ferulate, *p*-coumarate, vanillin, vanillate,

4-hydroxybenzoate, protocatechuate, syringaldehyde, or syringate as the sole source of carbon and energy (Figure 2A). The enrichment cultures were then grown to mid-log phase for gDNA extraction. Transposon-associated barcodes were amplified from each sample and sequenced, and the ratio of barcode counts between the selection and baseline conditions was used to determine a normalized gene fitness value for each nonessential gene under each selection condition (Figure 2; Table S3). Negative fitness values indicate that transposon-mediated disruption of the gene diminished growth relative to baseline (i.e., the gene was important for growth), while positive fitness values indicate that disruption of the gene improved growth relative to baseline (i.e., the gene hindered growth). Each gene fitness value was also associated with a *t*-like statistic for significance (Table S3; STAR Methods).

Known pathways for aromatic catabolism and associated fitness scores are presented in Figure 2. As expected, the hydroxylase gene *pobA* and its regulator *pobR* showed strongly negative fitness values for growth on *p*-coumarate and 4-hydroxybenzoate (H-type lignin-related compounds), but not for any other substrate. For G-type lignin-related compounds, genes with strongly negative fitness values included the vanillin dehydrogenase gene (*ligV*), the vanillate/3-*O*-methylgallate *O*-demethylase gene (*ligM*), the ferulate catabolic genes (*ferBA*), and genes in the tetrahydrofolate

(THF)-mediated C1 pathway (*metF*, *ligH*), which recycles THF as a cofactor for LigM and the syringate O-demethylase, DesA.<sup>48</sup> The *ferBA* genes also exhibited strongly negative fitness values for both *p*-coumarate and ferulate. The *ferB2* gene, which acts as a redundant copy of the *p*-hydroxycinnamoyl-coenzyme A (CoA) hydratase/lyase gene, did not exhibit strong fitness magnitudes under any condition tested, in agreement with prior observations that transcription levels of *ferB2* are <10% of *ferB* during growth on ferulate.<sup>49</sup> The MarR-type transcriptional regulator FerC is encoded just upstream of *ferB* and negatively regulates *ferBA* through induction by hydroxycinnamoyl-CoAs.<sup>49</sup> Surprisingly, *ferC* exhibited negative fitness for growth on ferulate but slightly positive fitness for growth on *p*-coumarate and syringate. For syringate, it is possible that readthrough from the *ferB* promoter positively affected the transcription of SLG\_25010-*desA*.<sup>36</sup>

All tested aromatic compounds require a common set of genes encoding ring cleavage pathway enzymes for funneling to central metabolism (*ligI*, *ligU*, *ligJ*, and *ligK*),<sup>50,51</sup> and each of these accordingly displayed large negative fitness values across conditions. LigR activates the transcription of *ligKUI* and *ligJABC* in the presence of protocatechuate or gallate,<sup>52</sup> and *ligR* showed negative fitness in all conditions. The 4-carboxy-2-hydroxy-6-semialdehyde (CHMS) dehydrogenase gene, *ligC*,<sup>53</sup> did not contain more than five transposon insertions in any sample, so it did not qualify for fitness analysis and may therefore exhibit a degree of essentiality in SYK-6. Additionally, the open reading frame (ORF) between *ligR* and *ligJ*, SLG\_12530, did not exhibit strong fitness magnitude in any condition despite its colocalization with the *lig* genes (Table S3). Prior studies<sup>52,54</sup> reported that SLG\_12530 was not translated in the presence of protocatechuate and its disruption did not affect growth on vanillate or syringate, indicating that the RB-TnSeq experiments successfully differentiated important catabolic genes on a per-gene basis.

The protocatechuate 4,5-dioxygenase genes, *ligAB*, showed strong negative fitness values for all conditions except those for S-type lignin-related compounds. Indeed, syringate and syringaldehyde are both catabolized via 3-O-methylgallate, which may undergo cleavage via DesZ and LigAB or via LigM, DesB, and LigAB.<sup>55</sup> Fitness scores for growth on syringate and syringaldehyde were of low magnitude for most of the genes encoding these enzymes, reflecting pathway redundancy. However, especially for syringate, *ligM* and *desB* displayed large negative fitness scores, indicating a preference for the catabolic pathway through gallate over 2-pyrone-4,6-dicarboxylate (PDC). The MarR-type regulator of *ligM-metF-ligH* and *desB*, encoded by *desR*,<sup>56</sup> did not contain enough transposon insertions in the baseline condition to qualify for analysis, so it may be broadly important for growth. Finally, the gene encoding DesX, which negatively regulates transcription of *desA*, exhibited strong positive fitness during growth on syringate, suggesting that knockout of this repressor may enhance catabolic efficiency for syringate. The *desA* gene is co-transcribed in an operon with a relatively uncharacterized hydrolase, SLG\_25010, whose fitness values closely matched that of *desA* (Table S3), in agreement with the observation that transcription of both genes is up-regulated by syringate.<sup>36</sup>

### Comparison of enrichment conditions identifies genes important for DDVA catabolism

To quantify gene fitness in the catabolic pathway for DDVA, a model 5-5 lignin-related dimer, aliquots of the SYK-6 transposon mutant library were grown to mid-log phase in rich medium (LB) and then passaged into minimal medium supplemented with either DDVA or vanillate. Fitness calculations were performed between the enrichment condition and the baseline condition, and then average normalized gene fitness scores were compared for the two enrichment conditions (Figure 3A). This approach resolved enrichment-specific fitness effects from those shared for both substrates, such that shared fitness effects are observed along the  $y = x$  parity line, DDVA-specific fitness effects cluster along the  $x = 0$  line, and vanillate-specific effects are observed along the  $y = 0$  line (Figure 3B). Additionally, fitness scores between the two conditions were compared with a two-tailed t test for significance. These analytical approaches enabled resolution of genes with the greatest fitness differences between DDVA enrichment and vanillate enrichment (Figure 3C; Table S4).

Unsurprisingly, many of the most significant gene fitness values for growth on DDVA were associated with known DDVA catabolic genes (Figure 3D), including the DDVA transporters encoded by *ddvT* and *ddvK*,<sup>57,58</sup> the DDVA O-demethylase encoded by *ligXaXcXd*,<sup>35</sup> the ring cleavage enzyme encoded by *ligZ*, and the hydrolase encoded by *ligY*.<sup>59,60</sup> Notably, the TonB system genes *tonB1*, *exbB1*, *exbD1*, and *exbD2* (SLG\_14430–14460), which are suggested to be involved in DDVA transport,<sup>58</sup> did not contain any barcoded transposon insertions (Table S2), consistent with previous conclusions that *tonB1* is essential for growth in SYK-6.<sup>58</sup> Meanwhile, *ddvR*, which encodes the MarR-type transcriptional regulator of many DDVA catabolic genes (Figure 3E), exhibited an average normalized gene fitness value of only  $-0.44$  for enrichment on DDVA, and this was not significantly different from the fitness values for enrichment on vanillate. SYK-6 encodes redundant enzymes, *ligW* and *ligW2*, to catalyze the decarboxylation of 5-carboxyvanillate to vanillate, but only *ligW2* displayed a significant and negative fitness score for enrichment on DDVA (Figure 3D). This is in agreement with previous work, which showed that knockout of *ligW2* severely affected growth on DDVA compared to knockout of *ligW*.<sup>61</sup> Among genes with the greatest fitness differences between DDVA and vanillate enrichment, four lack any prior characterization (Figure 3C). Two of these, SLG\_07730 and SLG\_07740, are encoded in the DDVA catabolic genes cluster (Figure 3E). In agreement with their significant, negative fitness values, knockout of SLG\_07730 or SLG\_07740 in SYK-6 resulted in a growth defect with DDVA (Figures S1A–S1C). The product of SLG\_07730 is annotated as a dimethylmenaquinone methyltransferase, while the product of SLG\_07740 is annotated as a RraA family protein. Domain searches indicated that both gene products contain an RraA family domain (cd16841), which is also found in the CHA aldolase, LigK, of the protocatechuate 4,5-cleavage pathway. Additionally, in other Sphingomonadales, genes with homology to SLG\_07730 and SLG\_07740 tend to fall in the same gene neighborhood as genes encoding amidohydrolases such as LigJ. SLG\_07730 and SLG\_07740 may therefore be involved in the catabolism of CHPD, and future metabolic

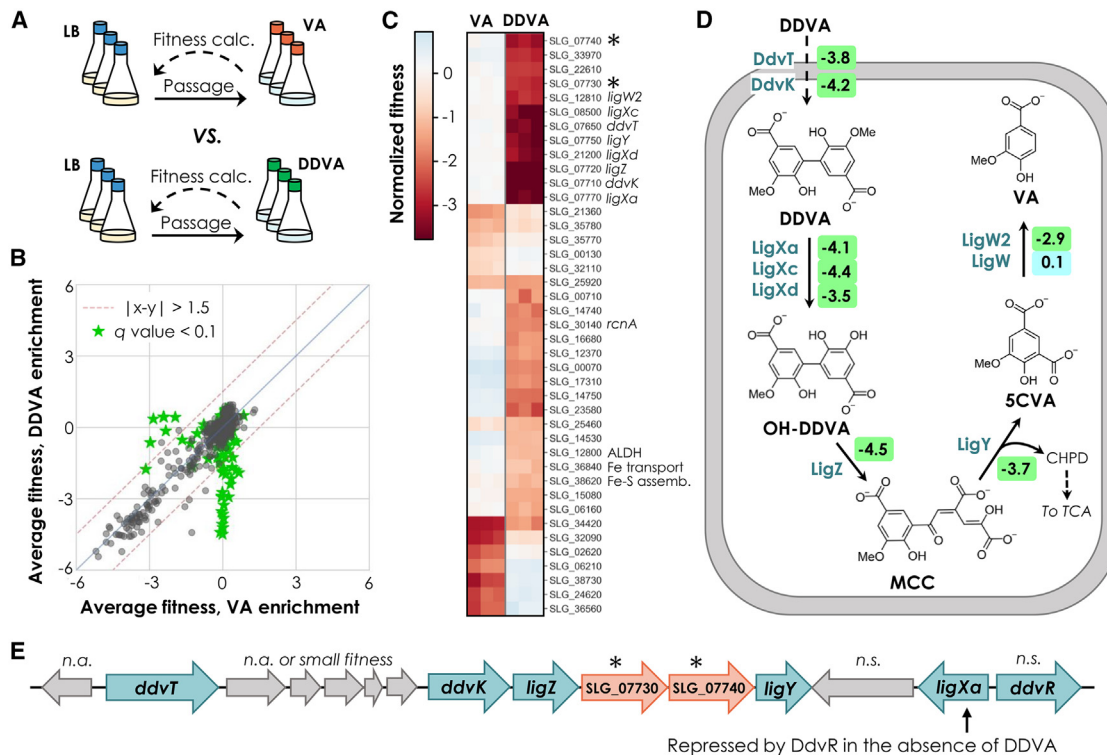


**Figure 3. Analysis of DDVA catabolism with the RB-TnSeq library in SYK-6**

(A and B) (A) Experimental design for identification of genes specifically involved in growth on DDVA but not VA. Fitness calculations were made between the enrichment condition (Wx minimal medium + 5 mM DDVA or 10 mM VA) and the baseline condition (LB medium), and then (B) average normalized gene fitness scores for these two enrichment conditions were compared. Genes with a specific fitness effect in the DDVA condition fall along the  $x = 0$  line. Red dashed lines indicate genes with a difference in average fitness score of more than 1.5, and green stars denote a significant ( $q < 0.1$ ) difference in fitness between the two conditions, as determined by a two-sample t test. Numerical data are provided in Table S4.

(C) A clustered heatmap of fitness scores for selected genes with a significant fitness difference ( $q < 0.1$ ) reveals the importance of DDVA catabolic genes for growth.

(D) Metabolic pathway for DDVA to VA in SYK-6, with participant enzymes labeled in blue text. Average normalized gene fitness scores are highlighted in green boxes when  $q < 0.1$  and in cyan boxes when  $q \geq 0.1$ .

(E) Genomic architecture of the DDVA catabolic genes cluster, whose genes are repressed in the absence of DDVA. n.a., failed to qualify for BarSeq analysis; small fitness, exhibited low fitness magnitude; n.s., not significant in the two-sample t test (see Table S3). In (C) and (E), genes marked with an asterisk exhibited significant fitness differences during growth on DDVA relative to VA. DDVA, 5,5'-dehydrodivanillate; OH-DDVA, 2,2',3-trihydroxy-3'-methoxy-5,5'-dicarboxy-biphenyl; MCC, 4,11-dicarboxy-8-hydroxy-9-methoxy-2-hydroxy-6-oxo-6-phenylhexa-2,4-dienoate; 5CVA, 5-carboxyvanillate; CHPD, 4-carboxy-2-hydroxypenta-2,4-dienoate.

engineering efforts should aim to fully define the role of these two genes in DDVA catabolism.

### RB-TnSeq enables resolution of significant genes in redundant $\beta$ -aryl ether catabolic pathways

Due to the abundance of  $\beta$ -O-4 linkages in the lignin polymer, guaiacylglycerol- $\beta$ -guaiacyl ether (GGE) was used as a model compound to study the catabolism of  $\beta$ -O-4-type dimers. SYK-6 can grow on GGE as the sole source of carbon and energy, albeit slowly (Figure S1D).<sup>62</sup> Similar to DDVA, normalized gene fitness values were determined for growth on GGE by passing aliquots of the SYK-6 transposon mutant library from rich medium into minimal medium containing either GGE (a racemic mixture of its four stereoisomers, with the majority in *erythro* form; see section “method details”) or vanillate (a downstream metabolite of GGE; Figure 4A). In doing so, fitness effects specific to GGE were thus resolved from those shared

between substrates by comparing the average fitness scores for growth on GGE to those for growth on vanillate (Figure 4B). Interestingly, few genes exhibited statistically significantly different fitness scores ( $q < 0.1$ ) between the two enrichment conditions (Table S4). Most catabolic genes for GGE are known, but many of the enzymes are stereospecific (Figure 4C). The RB-TnSeq experiments described here utilized a racemic mixture of GGE, so all these enzymes were likely important for growth and therefore exhibited dampened, nonsignificant fitness effects. The gene encoding HpvZ, however, exhibited significant, negative fitness during selection on GGE, in keeping with its role as a bottleneck in the GGE degradation pathway (Figure 4C).<sup>63</sup> More strikingly, SLG\_35860 exhibited a very high average fitness value in the GGE enrichment condition. This gene encodes a TetR family transcriptional regulator that is near the coding sequences for LigO and LigN (Figure 4D). The positive fitness value observed here for SLG\_35860 indicates that it may natively repress

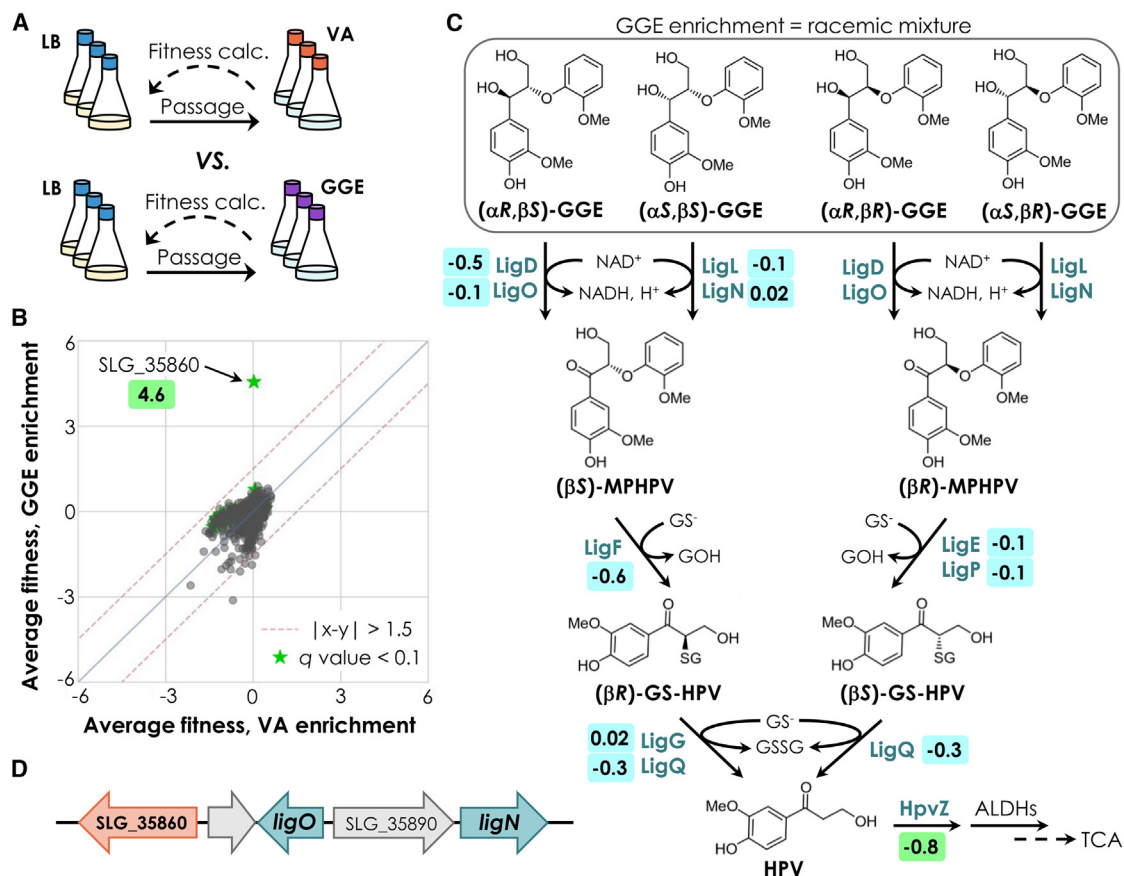


**Figure 4. Analysis of GGE catabolism highlights pathway redundancy**

(A and B) (A) The SYK-6 RB-TnSeq library was cultivated in triplicate in rich (LB) medium, and cells from each flask were passaged for enrichment in Wx minimal medium with either 1 mM VA or 1 mM GGE. Fitness calculations were made between each enrichment condition and the baseline condition, and then (B) average normalized gene fitness scores for the two enrichment conditions were compared. Genes with a specific fitness effect during growth with GGE fall along the  $x = 0$  line. Red dashed lines indicate genes with a difference in average fitness score of more than 1.5, and green stars denote a significant ( $q < 0.1$ ) difference in fitness between the two conditions, as determined by a two-sample t test. Numerical data are provided in Table S4.

(C) Catabolic pathways for GGE stereoisomers in SYK-6, with fitness scores for genes encoding each enzyme. The GGE substrate for enrichment of the SYK-6 transposon insertion library was a racemic mixture, so fitness scores were generally of small magnitude and not significant (cyan boxes). A significant fitness score (green box) was observed for *hpvZ*.

(D) The SLG\_35860 regulon likely includes *ligO* and *ligN*, as well as two undescribed genes (SLG\_35870, annotated as a hypothetical protein, and SLG\_35890, annotated as a TonB-dependent transporter). MPHPV,  $\alpha$ -(2-methoxyphenoxy)- $\beta$ -hydroxypropiovanillone; GS-HPV,  $\alpha$ -glutathionyl- $\beta$ -hydroxypropiovanillone; HPV,  $\beta$ -hydroxypropiovanillone; ALDHs, aldehyde dehydrogenases; GS<sup>-</sup>, reduced glutathione; GSSG, oxidized glutathione; GOH, guaiacol.

transcription of these and/or other GGE catabolic genes, such that its disruption leads to improved growth. Ongoing studies will examine SLG\_35860 as a metabolic engineering target to improve catabolism of GGE as well as other lignin-related aromatic dimers.

### RB-TnSeq reveals previously uncharacterized genes in $\beta$ -1 dimer catabolism

Multiple catalytic approaches to depolymerize the lignin polymer selectively cleave C–O bonds (e.g., the  $\beta$ -O-4 linkage found in GGE),<sup>3–5,64</sup> resulting in lignin streams enriched with C–C bonds, including dimers and oligomers that exhibit a ring-opened  $\beta$ -1 linkage.<sup>65,66</sup> Previous studies in *Novosphingobium aromaticivorans* DSM 12444, a bacterium with substantial aromatic catabolic pathway similarity to SYK-6, have demonstrated that this strain

can utilize 1,2-diguaiacylpropane-1,3-diol (DGPD), a model  $\beta$ -1 dimer,<sup>67,68</sup> but the same pathways have not been characterized with genome-wide experiments in SYK-6. To characterize gene function during growth on DGPD, the SYK-6 transposon mutant library was cultivated with isomers of the G-G  $\beta$ -1-type dimer, *erythro*-DGPD (eDGPD) and *threo*-DGPD (tDGPD), as well as isomers of the H-H  $\beta$ -1-type dimer, *erythro*-1,2-bis(*p*-hydroxyphenyl)propane-1,3-diol (eDHPD) and *threo*-DHPD (tDHPD), in Wx-SEMP medium in microtiter plates (Figures 5A and 5B). The *erythro* and *threo* forms each consist of two enantiomers ( $[\alpha S, \beta R]$  and  $[\alpha R, \beta S]$  for eDGPD;  $[\alpha S, \beta S]$  and  $[\alpha R, \beta R]$  for tDGPD; Figure 5C), but these were not separated for this study. Deformylation and dehydroxylation of DGPD produces one molar equivalent of lignostilbene in *N. aromaticivorans* and *Sphingomonas paucimobilis* TMY1009,<sup>67,69</sup> so lignostilbene

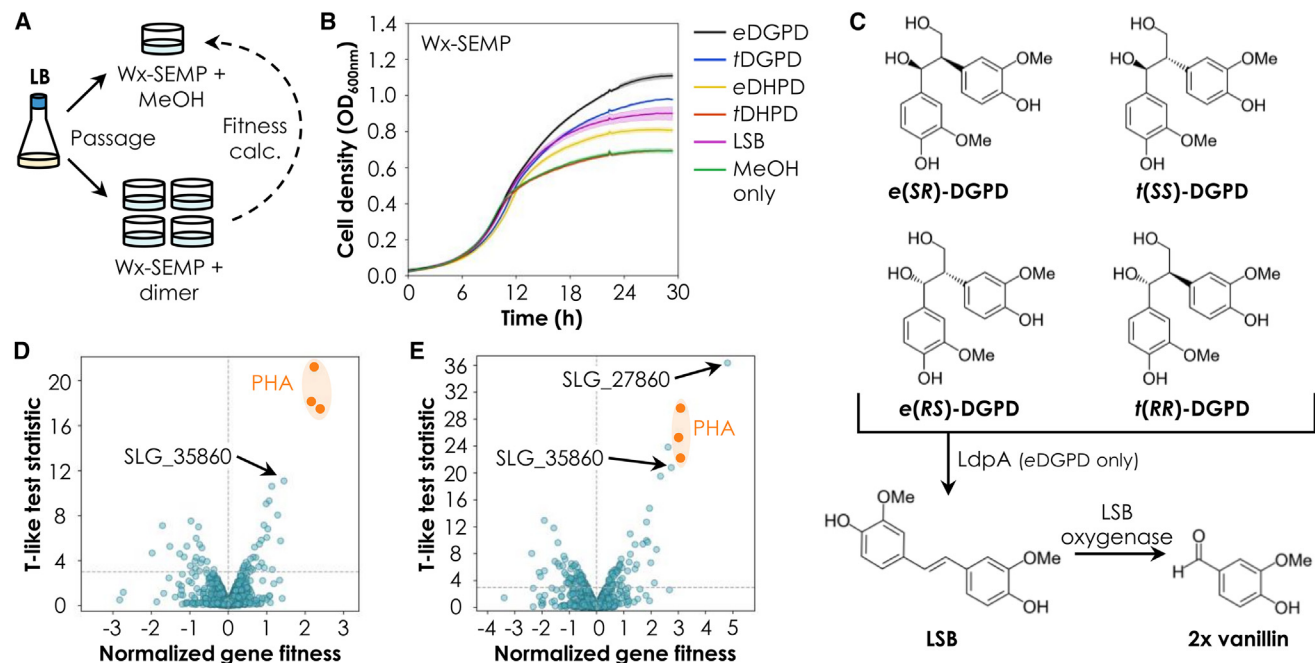


**Figure 5. RB-TnSeq identifies important genes for catabolism of DGPD, a  $\beta$ -1 dimer**

(A) The SYK-6 transposon mutant library was cultivated in rich (LB) medium and then inoculated into microtiter plates containing Wx-SEMP defined medium with 500  $\mu$ M  $\beta$ -1 dimer compound, 100  $\mu$ M lignostilbene, or the equivalent volume of the methanol solvent (MeOH). Wells were inoculated in triplicate, and cells from all three wells were pooled prior to gDNA extraction and BarSeq.

(B) Growth of the SYK-6 transposon mutant library on Wx-SEMP medium with  $\beta$ -1 dimers and related compounds. Assays were conducted in microtiter plates and error shading indicates standard deviation from the mean of three replicates.

(C–E) (C) A potential catabolic route for DGPD, based on homology. Volcano plots of normalized gene fitness scores were constructed for growth on (D) eDGPD and (E) tDGPD, where the t-like test statistic assesses how reliably each fitness value differs from 0. Genes with  $|t| > 3$  are plotted above the dashed gray line and considered to have stronger fitness effects. Orange highlighted dots indicate highly significant genes associated with PHA biosynthesis. The TetR family regulator gene, SLG\_35860, and winged helix DNA binding protein gene, SLG\_27860, are indicated with arrows. eDGPD, *erythro*-1,2-diguaiacylpropane-1,3-diol; tDGPD, *threo*-1,2-diguaiacylpropane-1,3-diol; eDHPD, *erythro*-1,2-bis(*p*-hydroxyphenyl)propane-1,3-diol; tDHPD, *threo*-1,2-bis(*p*-hydroxyphenyl)propane-1,3-diol; LSB, lignostilbene. DGPD has also been referred to as HMPPD, based on the International Union of Pure and Applied Chemistry (IUPAC) name, 1,2-bis(4-hydroxy-3-methoxyphenyl)-1,3-propanediol.

was included as a control (Figures 5B and 5C). All  $\beta$ -1-type model compounds were solvated in methanol, so growth of the library in Wx-SEMP medium with an equivalent volume of methanol was used as a baseline for fitness calculations. Except for tDHPD, all  $\beta$ -1-type dimers enabled enhanced growth relative to the methanol control (Figure 5B), indicating that these compounds were converted by SYK-6.

Fitness calculations were performed each growth condition, using the t-like test statistic as a measure of significance (see STAR Methods). Fitness scores were not determined for tDHPD due to lack of growth, and those for eDHPD exhibited low score magnitudes (Table S3). Aromatic catabolic genes were then investigated based on homology to previously characterized enzymes for G-G-type  $\beta$ -1 dimer catabolism. The product of SLG\_12650 (*ldpA*) shares 81% amino acid sequence identity with the enzyme that enables eDGPD degradation to lignostilbene in *N. aromaticivorans* (encoded by SARO\_2805; Figures 5C),<sup>67</sup> and *LdpA* has also been characterized biochemically.<sup>68</sup> The *ldpA* gene exhibited weakly negative fitness scores during growth on eDGPD and tDGPD, but not eDHPD or lignostilbene (Table S3), reflecting some specificity for the  $\beta$ -1 dimers. *N. aromaticivorans* also encodes a lignostilbene oxygenase

(*lsdA*; SARO\_2809) for cleavage of lignostilbene to two units of vanillin (Figure 5C).<sup>67</sup> In SYK-6, SLG\_12580 encodes an oxygenase with 55% identity to *LsdA*, but this gene did not exhibit strong fitness scores under any condition tested (Table S3). The lack of strong fitness scores for these catabolic genes may reflect pathway redundancy in SYK-6, which encodes eight *LsdA* homologs.<sup>70</sup>

For the G-G-type  $\beta$ -1 dimers (Figures 5D and 5E; Table S3), several genes exhibited strong positive fitness with high significance, including SLG\_35860 (TetR family transcriptional regulator), which also demonstrated positive fitness scores during cultivation with GGE (Figure 4B). Transposon-mediated disruption of this regulator may therefore enable transcription of multiple genes involved in the catabolism of a variety of aromatic oligomers related to lignin. When the library was grown on tDGPD, SLG\_27860 also showed a positive and very significant fitness score (Figure 5E). This gene is annotated as a winged helix DNA binding protein, which is a family that includes many well-conserved proteins typically involved in transcriptional regulation. SLG\_27860 is somewhat isolated in the SYK-6 genome, but it is upstream of the TonB-dependent transporter SLG\_27890, which was induced during degradation of DGPD

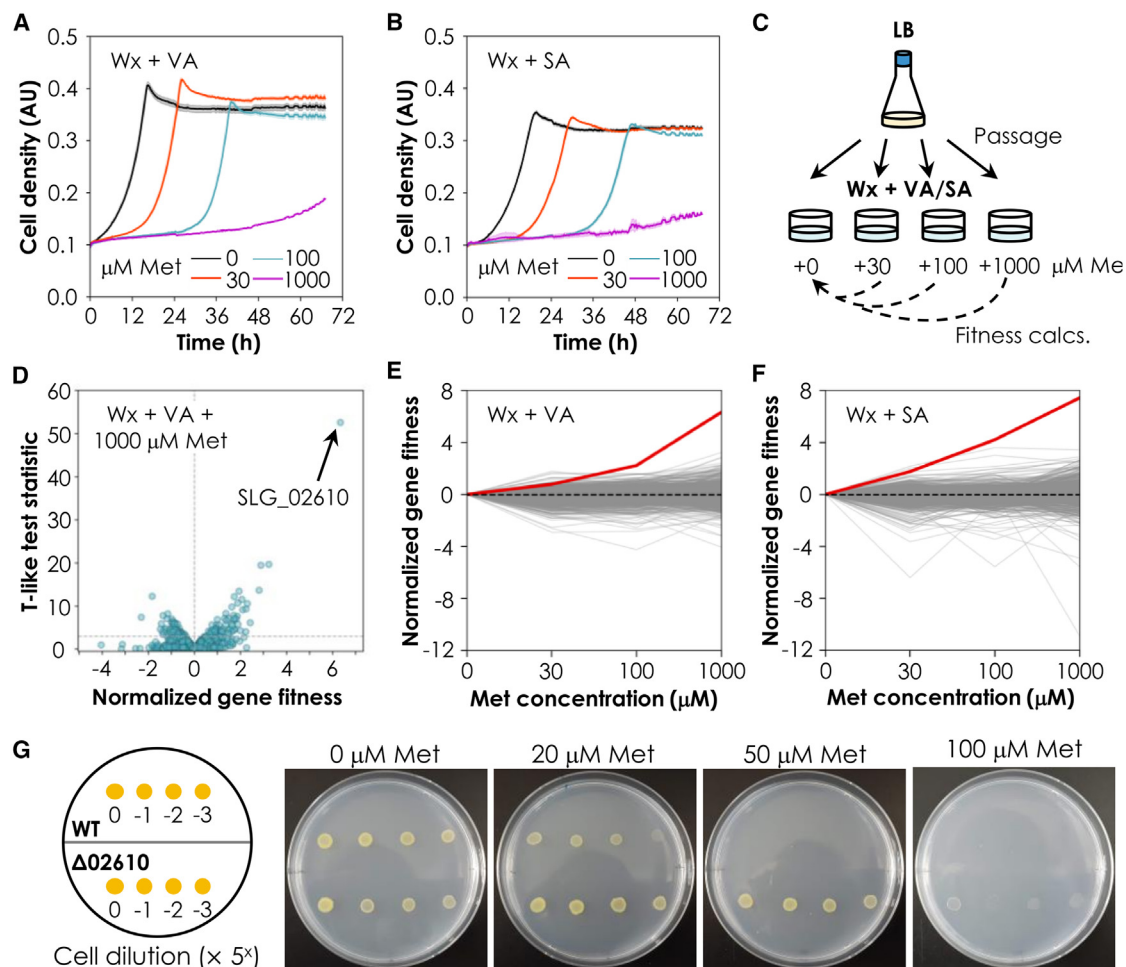


**Figure 6. Exogenous L-Met causes toxicity in wild-type SYK-6 in the presence of VA and syringate, and this effect is mitigated in a  $\Delta$ SLG\_02610 mutant**

(A and B) Growth in microtiter plates of wild-type SYK-6 on Wx minimal medium with 0, 30, 100, or 1,000  $\mu$ M L-Met and (A) 5 mM VA or (B) 5 mM syringate (SA). Error shading indicates the standard deviation from the mean of three replicates.

(C) The transposon mutant library of SYK-6 was cultivated in rich (LB) medium and then inoculated into microtiter plates containing Wx minimal medium with 5 mM VA or 5 mM SA and 30, 100, or 1,000  $\mu$ M L-Met. Wells were inoculated in triplicate, and then the cells from all three wells were pooled prior to gDNA extraction and BarSeq.

(D–F) (D) Volcano plot of t-like test statistics and normalized gene fitness values for all analyzed genes in the SYK-6 transposon mutant library after selection in Wx medium + 5 mM VA + 1,000  $\mu$ M L-Met. Gene SLG\_02610 exhibited the largest fitness magnitude (6.3) and t-like test statistic (52.6). Volcano plots for all other conditions are shown in Figures S1E–S1I. Plots of gene fitness as a function of L-Met concentration for growth of the SYK-6 transposon insertion library with (E) 5 mM VA or (F) 5 mM SA show increasingly positive fitness magnitude for SLG\_02610 (red lines).

(G) Agar plate growth assay for wild-type SYK-6 and the  $\Delta$ 02610 mutant, performed by plating serial 5-fold dilutions of each cell suspension on agar containing Wx minimal medium + 5 mM VA and 0–100  $\mu$ M L-Met. WT, wild type.

in a separate study.<sup>58</sup> Finally, both the eDGPD and tDGPD conditions produced very significant and positive fitness scores for genes involved in polyhydroxyalkanoate (PHA) biosynthesis (Figures 5D and 5E; Table S3). Disruption of SLG\_27860 and/or PHA biosynthetic genes may present an engineering opportunity to improve better growth on G-G-type  $\beta$ -1 dimers.

#### L-Met stress identifies an amino acid transporter

SYK-6 becomes an auxotroph for L-Met in the absence of compounds with an *O*-methyl group,<sup>71,72</sup> so L-Met must be supplemented to enable growth on aromatics such as *p*-coumarate

and 4-hydroxybenzoate. However, in the case of wild-type SYK-6 growth on *O*-methylated aromatics, such as vanillate and syringate, exogenous L-Met causes growth inhibition (Figures 6A and 6B). To investigate this toxicity effect, the RB-TnSeq library was cultivated in rich (LB) medium and then passaged in triplicate to wells of a microtiter plate containing Wx minimal medium supplemented with vanillate or syringate and increasing concentrations of L-Met (Figure 6C).

For growth in medium with L-Met and vanillate or syringate, most normalized gene fitness values clustered between magnitudes of 0 and 2 (Table S3), but one gene, SLG\_02610, exhibited

large positive fitness scores with remarkably high t-like test statistics across all conditions (Figure 6D; Figures S1E–S1I). The fitness of SLG\_02610 increased with increasing L-Met concentrations (Figures 6E and 6F), suggesting a relationship between gene function and L-Met metabolism. The gene product of SLG\_02610 is annotated as an amino acid permease. To investigate the function of the transporter and its involvement in uptake and subsequent toxicity of intracellular L-Met accumulation, a clean deletion of SLG\_02610 was generated in SYK-6, resulting in strain  $\Delta$ 02610 (Table S9). A complement plasmid for the deleted gene, pSEVA02610, was also constructed (Table S9). Wild-type SYK-6,  $\Delta$ 02610, and  $\Delta$ 02610(pSEVA02610) were cultivated overnight and then spotted in serial dilutions onto agar plates containing Wx minimal medium with 5 mM vanillate and 0–100  $\mu$ M L-Met. Visual inspection of the plates revealed stronger L-Met tolerance in  $\Delta$ 02610 than wild-type SYK-6 (Figure 6G), and complementation in  $\Delta$ 02610(pSEVA02610) resulted in a growth defect relative to an empty vector control (Figures S2A and S2B). These results indicated that overaccumulation of L-Met was due to a combination of intracellular L-Met production from 5-methyl-THF generated from O-demethylation of vanillate<sup>73</sup> as well as uptake of exogenous L-Met. Deletion of SLG\_02610 therefore may alleviate toxicity by reducing at least some uptake of exogenous L-Met. However,  $\Delta$ 02610 exhibited only a slight defect relative to wild type during growth on agar supplemented with 4-hydroxybenzoate and L-Met (Figure S2C), indicating the presence of secondary mechanism(s) for uptake of this conditionally essential amino acid. Three other putative amino acid permeases exist in the SYK-6 genome, and none of these displayed significant fitness scores during L-Met stress (Table S6), but they may play a secondary role in L-Met uptake.

### Trehalose biosynthesis genes improve acetate stress tolerance in SYK-6 and *P. putida*

Lignin-enriched streams that are derived from whole biomass (such as alkaline-pretreated liquor [APL]) for industrial bioprocessing often contain a substantial fraction of acetates from hemicellulose, which may inhibit bacterial growth and/or target compound production.<sup>10,74–79</sup> To investigate the acetate tolerance of wild-type SYK-6, the strain was cultivated in Wx-SEMP medium in microtiter plates with increasing concentrations of exogenous acetate (Figure 7A). Impressively, SYK-6 tolerated up to 250 mM acetate in the medium, albeit with significant growth defects, so an experiment with the transposon mutant library was designed to investigate gene function during acetate stress. The library was cultivated in triplicate in Wx-SEMP medium as the baseline condition, and then these cultures were passaged and enriched either in Wx-SEMP medium again or in Wx-SEMP medium with 200 mM acetate (Figure 7B). Cells were collected at mid-log phase and processed for BarSeq, which enabled comparison of gene fitness between the two enrichment conditions (Figure 7C). Most genes with large fitness magnitudes fell roughly along the  $y = x$  line of origin, indicating their general importance for growth in Wx-SEMP medium. However, a few genes exhibited significant ( $q < 0.1$ ) differences in fitness score between the two conditions (Table S4), including SLG\_04510 (*otsB*), which is annotated as a trehalose-6-phos-

phate phosphatase. In *Escherichia coli* and *Candida albicans*, trehalose-6-phosphate synthase and trehalose-6-phosphate phosphatase (*OtsAB* and *Tps1-2*, respectively) form a pathway for trehalose biosynthesis,<sup>80,81</sup> and these enzymes share features with those encoded by *otsBA* in SYK-6 (Figure S3A). Intracellular accumulation of trehalose has been shown to enhance tolerance to osmotic stress.<sup>82</sup> The significance of SLG\_04510 in RB-TnSeq indicated that the *otsBA* operon may function similarly for acetate tolerance in SYK-6.

To test this hypothesis, the *otsBA* operon from SYK-6 was translated to another aromatic catabolic bacterium, *P. putida* KT2440. *P. putida* lacks the *otsBA* pathway for trehalose biosynthesis,<sup>83</sup> and it cannot utilize trehalose as the sole source of carbon and energy (Figure S3B). Two engineered strains were designed for expression of *otsBA* in *P. putida*: strain ACB283 encodes the operon from SYK-6, which includes a third gene (SLG\_04500) between *otsB* and *otsA*, while strain ACB285 encodes the two-gene *otsBA* operon from *E. coli* (Figure 7D). To examine the effect of this trehalose biosynthesis pathway in *P. putida*, KT2440 wild type and ACB283 were cultivated in microtiter plates in M9 minimal medium with 0–200 mM acetate. As expected, high concentrations of acetate inhibited the growth of both strains relative to growth on glucose alone, but ACB283 exhibited a shorter lag time than KT2440 wild type at high acetate concentrations (Figures 7E and S4A). This effect was minor, but reproducible (Figures S3C–S3E), indicating that overexpression of the *otsB*:SLG\_04500:*otsA* operon from SYK-6 may contribute mild improvements in acetate tolerance. Interestingly, ACB285 displayed a growth defect in all conditions, including growth on glucose alone (Figure S4A). The three-gene operon (*otsB*:SLG\_04500:*otsA*) from SYK-6 may therefore be more amenable for heterologous expression in *P. putida* than the two-gene operon (*otsB*:*otsA*) from *E. coli*.

### DISCUSSION

The RB-TnSeq approach described here for SYK-6 afforded multiplexed measurements of gene fitness across a variety of conditions related to aromatic catabolism. This validated known pathways for SYK-6 metabolism, while detailed analysis of gene fitness scores also revealed new aspects of aromatic catabolism in this model bacterium. The results in this study reflect only a modicum of potential for these datasets, and comparisons between enrichment conditions can identify genes with unique fitness scores in one condition but not the other. For example, selection experiments on syringate and vanillate identified a group of genes with negative fitness scores and high significance ( $q < 0.1$ ; Figure S5). Their products were annotated as molybdenum cofactor biosynthesis proteins (e.g., *MoA*E) and formate dehydrogenase (*FdhF*; Tables S3 and S7). Assimilation of syringate and vanillate requires O-demethylation and transfer of the methoxy-derived methyl group to a THF cofactor, which is regenerated by releasing formate and ultimately CO<sub>2</sub> via *FdhF*.<sup>48,71</sup> *FdhFs* are known to utilize a molybdenum cofactor,<sup>84</sup> so overexpression of this gene group in SYK-6 may enhance catabolism of S- and G-type lignin-related compounds by improving cofactor availability. In another example, an operon of four efflux transporter genes (SLG\_34600–34630) exhibited

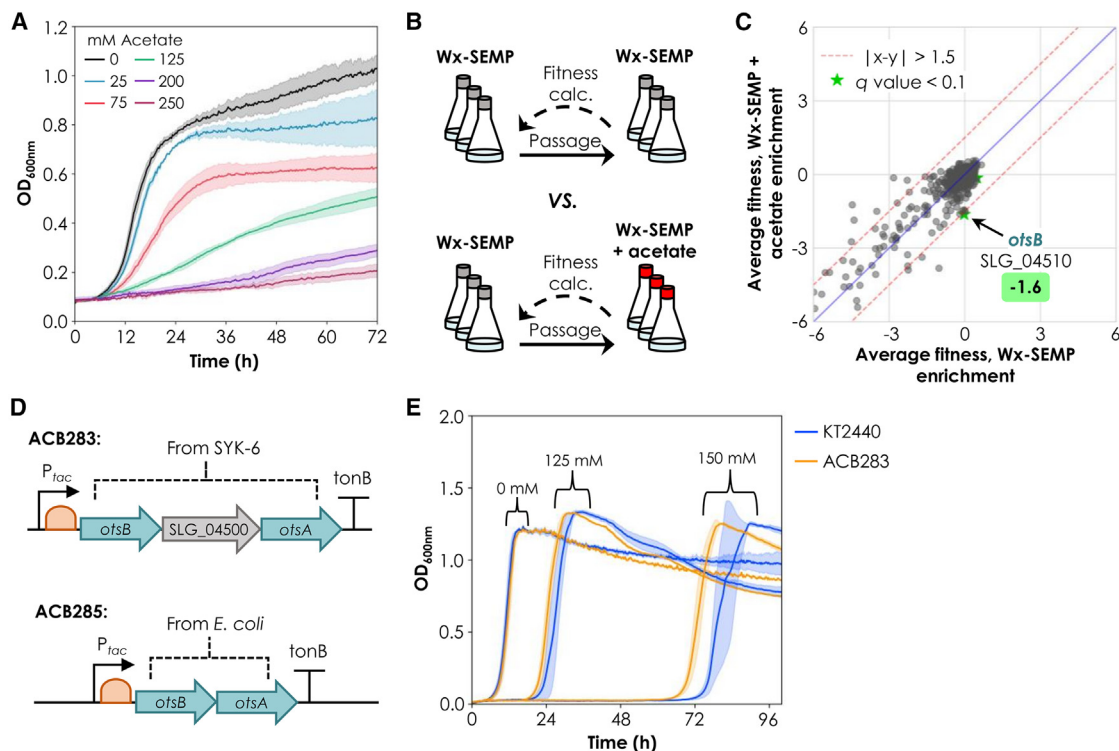


**Figure 7. The *otsBA* operon may mitigate acetate stress in SYK-6 and *P. putida***

(A) Increased supplementation of acetate led to decreased growth of wild-type SYK-6 in Wx-SEMP defined medium.

(B and C) (B) The SYK-6 RB-TnSeq library was cultivated in triplicate in Wx-SEMP medium, and cells from each flask were passed for enrichment in Wx-SEMP with or without 200 mM acetate. Fitness calculations were made between each enrichment condition and the baseline condition, and then (C) average normalized gene fitness scores for the two enrichment conditions were compared. Genes with a specific fitness effect during acetate stress fall along the  $x = 0$  line. Red dashed lines indicate genes with a difference in average fitness score of more than 1.5, and green stars denote a significant ( $q < 0.1$ ) difference in fitness between the two conditions, as determined by a two-sample t test. Numerical data are provided in Table S4.

(D) Expression of the *otsBA* operons from SYK-6 (top) and *E. coli* B (bottom) in *P. putida* strains ACB283 and ACB285, respectively. The SYK-6 *otsBA* operon includes a third gene, SLG\_04500.

(E) Growth of *P. putida* KT2440 wild type and ACB283 in M9 + 20 mM glucose with 0, 125, or 150 mM acetate. Error shadings in (A) and (E) indicate the standard deviation from the mean of three biological replicates. One replicate of KT2440 wild type failed to grow in the presence of 150 mM acetate after 200 h, so it was not included for clarity.

significant and positive fitness values during selection on vanillin compared to vanillate (Tables S3 and S8), indicating that disruption of the efflux system may retain vanillin in the cell, thereby improving its assimilation. Finally, the SLG\_25740 LysR family transcriptional regulator exhibited negative and significant fitness scores during enrichment on S- and G-type lignin-related compounds (Table S3), and it is located near *metB*, so it may play a role in regulating L-Met biosynthesis. Deep examination of RB-TnSeq data such as these can generate hypotheses that encourage further experimental validation of potential gene functions in SYK-6.

RB-TnSeq also aided analysis of lignin-related dimer catabolism. During DDVA enrichment, strong negative fitness scores were observed for the previously undescribed SLG\_07730 and SLG\_07740 genes (Figures 3C and 3E). Enrichment on DDVA also highlighted a fitness effect for two other uncharacterized genes. The product of SLG\_33970 is implicated in guanosine 3'-diphosphate 5'-di(tri)phosphate ((p)ppGpp) biosynthesis, which may regulate gene expression during the stringent

response,<sup>85</sup> and the product of SLG\_22610 is predicted to integrate in the membrane. Several other genes, including an aldehyde dehydrogenase (ALDH), *rcnA*, and two genes involved in iron transport and iron-sulfur cluster assembly (Figure 3C), exhibited significantly different fitness scores during enrichment on DDVA compared to vanillate. Further investigation is required to explain these strong fitness effects and evaluate their potential as metabolic engineering targets. Additional validation is also needed to explain some strong fitness changes during enrichment on GGE, such as SLG\_34620, which is annotated as an RND efflux transporter with 53% identity to MexF in *P. putida* and 51% identity to multidrug efflux transporter OqxB from *Klebsiella pneumoniae*, so it may be involved with the efflux of toxic substrates or metabolites that accumulate in the cell.<sup>86</sup> Together, these previously uncharacterized genes should be considered in the design of dimer catabolic pathways, either for optimization in SYK-6 or for heterologous expression in another lignin-relevant host, as has been demonstrated for the  $\beta$ -1 dimer DGPD in *P. putida*.<sup>67</sup>

Analysis of the RB-TnSeq library in SYK-6 also provided insights to tolerance. Growth defects on vanillate and syringate in the presence of L-Met may be mitigated by disruption of SLG\_02610, which shares 50% sequence identity with a structurally characterized cationic amino acid transporter from *Geobacillus kaustophilus*.<sup>87</sup> However, knockout of SLG\_02610 does not fully abrogate growth on non-methoxylated compounds such as 4-hydroxybenzoate, so other L-Met transporters or nonspecific transporters likely exist.

Process engineering strategies for reducing acetate inhibition in biorefinery applications include acetate removal or simply feeding substrates such as APL at a lower rate, but these can increase process costs and decrease bioprocess performance.<sup>74</sup> Genetic engineering therefore represents an appealing strategy to overcome acetate stress without the need for major process adjustments. In this study, RB-TnSeq identified the importance of SLG\_04510 (*otsB*) for growth in the presence of acetate, and heterologous expression of the *otsB*:SLG\_04500:*otsA* trehalose biosynthesis operon conferred improved acetate tolerance in *P. putida* strain ACB283 (Figure 7E). However, expression of an *otsB*:*otsA* ortholog from *E. coli* hindered growth of *P. putida* strain ACB285, even on glucose alone. In KT2440, glucose flux is mostly through gluconate and 6-phosphogluconate,<sup>88</sup> resulting in less glucose-6-phosphate production. OtsA utilizes glucose-6-phosphate that would otherwise enter glycolysis (Figure S4B), so high amounts of OtsAB in the cytoplasm may compete with the enzymes necessary for growth on glucose, leading to the growth defects observed for ACB285. Meanwhile, no growth defects were observed for ACB283 on glucose, so expression of the middle operon gene (SLG\_04500, a glycoside hydrolase) may mitigate competition with glycolysis in *P. putida*. These effects are also likely confounded by the presence of additional trehalose biosynthesis and degradation pathways in *P. putida*,<sup>83</sup> which we did not modify in this study. Further understanding of trehalose metabolism and regulation in SYK-6 and *P. putida* is therefore needed to effectively leverage this mechanism for acid tolerance, but the demonstration here with strain ACB283 could provide a foundation for future engineering efforts.

### Limitations of the study

In this study, we generated a randomly barcoded transposon mutant insertion library in the aromatic catabolic bacterium SYK-6. The library is of high quality, with deep coverage and insertions in over 90% of protein-coding genes. Genes without insertions may represent essential genes, and combination of this information with knockdown approaches such as CRISPR interference (CRISPRi) could clarify the importance of these genes.<sup>89</sup> A variety of enrichment conditions were applied to quantify gene fitness by RB-TnSeq, and the findings could be further applied to optimize SYK-6 metabolism or express SYK-6 pathways in other organisms with the goal of improving catabolism of lignin-related aromatic compounds. The fitness assays here were restricted to pure aromatic compounds and stress conditions, but the library could be propagated and re-used for additional mutant fitness assays, including mixed substrate streams derived from lignin (e.g., APL), other lignin-relevant aromatic compounds, or substrates with relevance to other applications. This would expand

knowledge of SYK-6 metabolism beyond the relatively simple studies described here for model compounds. Finally, gene fitness data from RB-TnSeq experiments could be combined with other -omics datasets<sup>43</sup> to further elucidate relationships between gene function and environment.

### STAR★METHODS

Detailed methods are provided in the online version of this paper and include the following:

- KEY RESOURCES TABLE
- RESOURCE AVAILABILITY
  - Lead contact
  - Materials availability
  - Data and code availability
- EXPERIMENTAL MODEL AND SUBJECT DETAILS
- METHOD DETAILS
  - Generation of a randomly barcoded Tn5 transposon mutant library in SYK-6
  - Preparation of the transposon mutant library for sequencing
  - TnSeq data analysis
  - Competitive mutant fitness assays
  - Preparation of samples for BarSeq
  - Fitness analysis
  - Bacterial strains, plasmids, and culture conditions
  - Growth assays for SYK-6 and engineered mutants thereof
  - Growth assays for *P. putida* and engineered mutants thereof
  - Compound preparation and sourcing
- QUANTIFICATION AND STATISTICAL ANALYSIS

### SUPPLEMENTAL INFORMATION

Supplemental information can be found online at <https://doi.org/10.1016/j.celrep.2023.112847>.

### ACKNOWLEDGMENTS

The authors thank Adam Deutschbauer and associates at the Joint Genome Institute for the pKMW7 barcoded Tn5 transposon vector library (APA766), the laboratory of Lindsay Eltis (University of British Columbia) for the lignostilbene compound, and Adam Guss and Joshua Elmore (Oak Ridge National Laboratory) for donation of strain AG4775. We thank Andrew J. Borchert for assistance with code de-bugging and productive discussions.

This work was partially authored by the Alliance for Sustainable Energy, LLC, the manager and operator of the National Renewable Energy Laboratory for the US Department of Energy (DOE), under contract no. DE-AC36-08GO28308. A.B., Z.A.K., and G.T.B. were funded by The Center for Bioenergy Innovation, a US DOE Bioenergy Research Center supported by the Office of Biological and Environmental Research in the DOE Office of Science. Funding for organic synthesis was provided to R. Katahira and G.T.B. by the DOE Office of Energy Efficiency and Renewable Energy Bioenergy Technologies Office. E.M. was funded by JSPS KAKENHI grant number 19H02867.

### AUTHOR CONTRIBUTIONS

Conceptualization, A.B., E.M., and G.T.B.; methodology and software, data curation, writing – original draft, and visualization, A.B.; formal analysis, A.B. and Z.A.K.; investigation, A.B., R. Kato, Z.A.K., and M.M.; resources, R.

Katahira; writing – review & editing, A.B., N.K., E.M., and G.T.B.; funding acquisition, E.M. and G.T.B.

#### DECLARATION OF INTERESTS

The authors declare no competing interests.

#### INCLUSION AND DIVERSITY

We support inclusive, diverse, and equitable conduct of research.

Received: November 28, 2022

Revised: May 21, 2023

Accepted: July 7, 2023

#### REFERENCES

- Bruijninx, P.C.A., Rinaldi, R., and Weckhuysen, B.M. (2015). Unlocking the potential of a sleeping giant: lignins as sustainable raw materials for renewable fuels, chemicals and materials. *Green Chem.* *17*, 4860–4861. <https://doi.org/10.1039/C5GC90055G>.
- Weiland, F., Kohlstedt, M., and Wittmann, C. (2022). Guiding stars to the field of dreams: Metabolically engineered pathways and microbial platforms for a sustainable lignin-based industry. *Metab. Eng.* *71*, 13–41. <https://doi.org/10.1016/j.ymben.2021.11.011>.
- Rinaldi, R., Jastrzebski, R., Clough, M.T., Ralph, J., Kennema, M., Bruijninx, P.C.A., and Weckhuysen, B.M. (2016). Paving the way for lignin valorisation: recent advances in bioengineering, biorefining and catalysis. *Angew. Chem. Int. Ed.* *55*, 8164–8215. <https://doi.org/10.1002/anie.201510351>.
- Schutyser, W., Renders, T., Van den Bosch, S., Koelewijn, S.-F., Beckham, G.T., and Sels, B.F. (2018). Chemicals from lignin: an interplay of lignocellulose fractionation, depolymerisation, and upgrading. *Chem. Soc. Rev.* *47*, 852–908. <https://doi.org/10.1039/C7CS00566K>.
- Sun, Z., Fridrich, B., de Santi, A., Elangovan, S., and Barta, K. (2018). Bright side of lignin depolymerization: toward new platform chemicals. *Chem. Rev.* *118*, 614–678. <https://doi.org/10.1021/acs.chemrev.7b00588>.
- del Río, J.C., Rencoret, J., Gutiérrez, A., Elder, T., Kim, H., and Ralph, J. (2020). Lignin monomers from beyond the canonical monolignol biosynthetic pathway: another brick in the wall. *ACS Sustain. Chem. Eng.* *8*, 4997–5012. <https://doi.org/10.1021/acssuschemeng.0c01109>.
- Jiménez, J.I., Miñambres, B., García, J.L., and Díaz, E. (2002). Genomic analysis of the aromatic catabolic pathways from *Pseudomonas putida* KT2440. *Environ. Microbiol.* *4*, 824–841. <https://doi.org/10.1046/j.1462-2920.2002.00370.x>.
- Shen, X.-H., Zhou, N.-Y., and Liu, S.-J. (2012). Degradation and assimilation of aromatic compounds by *Corynebacterium glutamicum*: another potential for applications for this bacterium? *Appl. Microbiol. Biotechnol.* *95*, 77–89. <https://doi.org/10.1007/s00253-012-4139-4>.
- Linger, J.G., Vardon, D.R., Guarnieri, M.T., Karp, E.M., Hunsinger, G.B., Franden, M.A., Johnson, C.W., Chupka, G., Strathmann, T.J., Pienkos, P.T., and Beckham, G.T. (2014). Lignin valorization through integrated biological funneling and chemical catalysis. *Proc. Natl. Acad. Sci. USA* *111*, 12013–12018. <https://doi.org/10.1073/pnas.1410657111>.
- Salvachúa, D., Karp, E.M., Nimlos, C.T., Vardon, D.R., and Beckham, G.T. (2015). Towards lignin consolidated bioprocessing: simultaneous lignin depolymerization and product generation by bacteria. *Green Chem.* *17*, 4951–4967. <https://doi.org/10.1039/C5GC01165E>.
- Kamimura, N., Takahashi, K., Mori, K., Araki, T., Fujita, M., Higuchi, Y., and Masai, E. (2017). Bacterial catabolism of lignin-derived aromatics: New findings in a recent decade: Update on bacterial lignin catabolism. *Environ. Microbiol. Rep.* *9*, 679–705. <https://doi.org/10.1111/1758-2229.12597>.
- Ravi, K., García-Hidalgo, J., Gorwa-Grauslund, M.F., and Lidén, G. (2017). Conversion of lignin model compounds by *Pseudomonas putida* KT2440 and isolates from compost. *Appl. Microbiol. Biotechnol.* *101*, 5059–5070. <https://doi.org/10.1007/s00253-017-8211-y>.
- Wilhelm, R.C., Singh, R., Eltis, L.D., and Mohn, W.W. (2019). Bacterial contributions to delignification and lignocellulose degradation in forest soils with metagenomic and quantitative stable isotope probing. *ISME J.* *13*, 413–429. <https://doi.org/10.1038/s41396-018-0279-6>.
- Navas, L.E., Dexter, G., Liu, J., Levy-Booth, D., Cho, M., Jang, S.-K., Mansfield, S.D., Renneckar, S., Mohn, W.W., and Eltis, L.D. (2021). Bacterial transformation of aromatic monomers in softwood black liquor. *Front. Microbiol.* *12*, 735000. <https://doi.org/10.3389/fmicb.2021.735000>.
- Erickson, E., Bleem, A., Kuatsjah, E., Werner, A.Z., DuBois, J.L., McGeehan, J.E., Eltis, L.D., and Beckham, G.T. (2022). Critical enzyme reactions in aromatic catabolism for microbial lignin conversion. *Nat. Catal.* *5*, 86–98. <https://doi.org/10.1038/s41929-022-00747-w>.
- Barton, N., Horbal, L., Starck, S., Kohlstedt, M., Luzhetskyy, A., and Wittmann, C. (2018). Enabling the valorization of guaiacol-based lignin: Integrated chemical and biochemical production of *cis,cis*-muconic acid using metabolically engineered *Amycolatopsis* sp. ATCC 39116. *Metab. Eng.* *45*, 200–210. <https://doi.org/10.1016/j.ymben.2017.12.001>.
- Becker, J., Kuhl, M., Kohlstedt, M., Starck, S., and Wittmann, C. (2018). Metabolic engineering of *Corynebacterium glutamicum* for the production of *cis,cis*-muconic acid from lignin. *Microb. Cell Fact.* *17*, 115. <https://doi.org/10.1186/s12934-018-0963-2>.
- Perez, J.M., Kontur, W.S., Alherech, M., Coplien, J., Karlen, S.D., Stahl, S.S., Donohue, T.J., and Noguera, D.R. (2019). Funneling aromatic products of chemically depolymerized lignin into 2-pyrone-4,6-dicarboxylic acid with *Novosphingobium aromaticivorans*. *Green Chem.* *21*, 1340–1350. <https://doi.org/10.1039/C8GC03504K>.
- Salvachúa, D., Rydzak, T., Auwae, R., De Capite, A., Black, B.A., Bouvier, J.T., Cleveland, N.S., Elmore, J.R., Huenemann, J.D., Katahira, R., et al. (2020). Metabolic engineering of *Pseudomonas putida* for increased polyhydroxyalkanoate production from lignin. *Microb. Biotechnol.* *13*, 290–298. <https://doi.org/10.1111/1751-7915.13481>.
- Arvay, E., Biggs, B.W., Guerrero, L., Jiang, V., and Tyo, K. (2021). Engineering *Acinetobacter baylyi* ADP1 for mevalonate production from lignin-derived aromatic compounds. *Metab. Eng. Commun.* *13*, e00173. <https://doi.org/10.1016/j.mec.2021.e00173>.
- Bugg, T.D., Williamson, J.J., and Alberti, F. (2021). Microbial hosts for metabolic engineering of lignin bioconversion to renewable chemicals. *Renew. Sustain. Energy Rev.* *152*, 111674. <https://doi.org/10.1016/j.rser.2021.111674>.
- Beckham, G.T., Johnson, C.W., Karp, E.M., Salvachúa, D., and Vardon, D.R. (2016). Opportunities and challenges in biological lignin valorization. *Curr. Opin. Biotechnol.* *42*, 40–53. <https://doi.org/10.1016/j.copbio.2016.02.030>.
- Masai, E., Katayama, Y., and Fukuda, M. (2007). Genetic and biochemical investigations on bacterial catabolic pathways for lignin-derived aromatic compounds. *Biosci. Biotechnol. Biochem.* *71*, 1–15. <https://doi.org/10.1271/bbb.60437>.
- Bugg, T.D.H., Ahmad, M., Hardiman, E.M., and Singh, R. (2011). The emerging role for bacteria in lignin degradation and bio-product formation. *Curr. Opin. Biotechnol.* *22*, 394–400. <https://doi.org/10.1016/j.copbio.2010.10.009>.
- Katayama, Y., Nishikawa, S., Murayama, A., Yamasaki, M., Morohoshi, N., and Haraguchi, T. (1988). The metabolism of biphenyl structures in lignin by the soil bacterium *Pseudomonas paucimobilis* SYK-6). *FEBS Lett.* *233*, 129–133. [https://doi.org/10.1016/0014-5793\(88\)81369-3](https://doi.org/10.1016/0014-5793(88)81369-3).
- Noda, Y., Nishikawa, S., Shiozuka, K., Kadokura, H., Nakajima, H., Yoda, K., Katayama, Y., Morohoshi, N., Haraguchi, T., and Yamasaki, M. (1990). Molecular cloning of the protocatechuate 4,5-dioxygenase genes of *Pseudomonas paucimobilis*. *J. Bacteriol.* *172*, 2704–2709. <https://doi.org/10.1128/jb.172.5.2704-2709.1990>.

27. Masai, E., Kamimura, N., Kasai, D., Oguchi, A., Ankai, A., Fukui, S., Takahashi, M., Yashiro, I., Sasaki, H., Harada, T., et al. (2012). Complete genome sequence of *Sphingobium* sp. strain SYK-6, a degrader of lignin-derived biaryls and monoaryls. *J. Bacteriol.* *194*, 534–535. <https://doi.org/10.1128/JB.06254-11>.
28. Otsuka, Y., Nakamura, M., Shigehara, K., Sugimura, K., Masai, E., Ohara, S., and Katayama, Y. (2006). Efficient production of 2-pyrone 4,6-dicarboxylic acid as a novel polymer-based material from protocatechuate by microbial function. *Appl. Microbiol. Biotechnol.* *71*, 608–614. <https://doi.org/10.1007/s00253-005-0203-7>.
29. Higuchi, Y., Kato, R., Tsubota, K., Kamimura, N., Westwood, N.J., and Masai, E. (2019). Discovery of novel enzyme genes involved in the conversion of an arylglycerol- $\beta$ -aryl ether metabolite and their use in generating a metabolic pathway for lignin valorization. *Metab. Eng.* *55*, 258–267. <https://doi.org/10.1016/j.ymben.2019.08.002>.
30. Johnson, C.W., Salvachúa, D., Rorrer, N.A., Black, B.A., Vardon, D.R., St John, P.C., Cleveland, N.S., Dominick, G., Elmore, J.R., Grundl, N., et al. (2019). Innovative chemicals and materials from bacterial aromatic catabolic pathways. *Joule* *3*, 1523–1537. <https://doi.org/10.1016/j.joule.2019.05.011>.
31. Notonier, S., Werner, A.Z., Kuatsjah, E., Dumalo, L., Abraham, P.E., Hatmaker, E.A., Hoyt, C.B., Amore, A., Ramirez, K.J., Woodworth, S.P., et al. (2021). Metabolism of syringyl lignin-derived compounds in *Pseudomonas putida* enables convergent production of 2-pyrone-4,6-dicarboxylic acid. *Metab. Eng.* *65*, 111–122. <https://doi.org/10.1016/j.ymben.2021.02.005>.
32. Otsuka, Y., Araki, T., Suzuki, Y., Nakamura, M., Kamimura, N., and Masai, E. (2023). High-level production of 2-pyrone-4,6-dicarboxylic acid from vanillic acid as a lignin-related aromatic compound by metabolically engineered fermentation to realize industrial valorization processes of lignin. *Bioresour. Technol.* *377*, 128956. <https://doi.org/10.1016/j.biortech.2023.128956>.
33. Masai, E., Harada, K., Peng, X., Kitayama, H., Katayama, Y., and Fukuda, M. (2002). Cloning and characterization of the ferulic acid catabolic genes of *Sphingomonas paucimobilis* SYK-6. *Appl. Environ. Microbiol.* *68*, 4416–4424. <https://doi.org/10.1128/aem.68.9.4416-4424.2002>.
34. Masai, E., Yamamoto, Y., Inoue, T., Takamura, K., Hara, H., Kasai, D., Katayama, Y., and Fukuda, M. (2007). Characterization of *ligV* essential for catabolism of vanillin by *Sphingomonas paucimobilis* SYK-6. *Biosci. Biotechnol. Biochem.* *71*, 2487–2492. <https://doi.org/10.1271/bbb.70267>.
35. Yoshikata, T., Suzuki, K., Kamimura, N., Namiki, M., Hishiyama, S., Araki, T., Kasai, D., Otsuka, Y., Nakamura, M., Fukuda, M., et al. (2014). Three-component O-demethylase system essential for catabolism of a lignin-derived biphenyl compound in *Sphingobium* sp. strain SYK-6. *Appl. Environ. Microbiol.* *80*, 7142–7153. <https://doi.org/10.1128/AEM.02236-14>.
36. Araki, T., Tanatani, K., Kamimura, N., Otsuka, Y., Yamaguchi, M., Nakamura, M., and Masai, E. (2020). The syringate O-demethylase gene of *Sphingobium* sp. strain SYK-6 is regulated by DesX, while other vanillate and syringate catabolism genes are regulated by DesR. *Appl. Environ. Microbiol.* *86*, e01712-20. <https://doi.org/10.1128/AEM.01712-20>.
37. Higuchi, Y., Sato, D., Kamimura, N., and Masai, E. (2020). Roles of two glutathione S-transferases in the final step of the  $\beta$ -aryl ether cleavage pathway in *Sphingobium* sp. strain SYK-6. *Sci. Rep.* *10*, 20614. <https://doi.org/10.1038/s41598-020-77462-8>.
38. Wetmore, K.M., Price, M.N., Waters, R.J., Lamson, J.S., He, J., Hoover, C.A., Blow, M.J., Bristow, J., Butland, G., Arkin, A.P., and Deutschbauer, A. (2015). Rapid quantification of mutant fitness in diverse bacteria by sequencing randomly bar-coded transposons. *mBio* *6*, e00306–e00315. <https://doi.org/10.1128/mBio.00306-15>.
39. Luneau, J.S., Baudin, M., Quiroz Monnens, T., Carrère, S., Bouchez, O., Jardinaud, M.F., Gris, C., François, J., Ray, J., Torralba, B., et al. (2022). Genome-wide identification of fitness determinants in the *Xanthomonas campestris* bacterial pathogen during early stages of plant infection. *New Phytol.* *236*, 235–248. <https://doi.org/10.1111/nph.18313>.
40. Price, M.N., Wetmore, K.M., Waters, R.J., Callaghan, M., Ray, J., Liu, H., Kuehl, J.V., Melnyk, R.A., Lamson, J.S., Suh, Y., et al. (2018). Mutant phenotypes for thousands of bacterial genes of unknown function. *Nature* *557*, 503–509. <https://doi.org/10.1038/s41586-018-0124-0>.
41. Cecil, J.H., Garcia, D.C., Giannone, R.J., and Michener, J.K. (2018). Rapid, parallel identification of catabolism pathways of lignin-derived aromatic compounds in *Novosphingobium aromaticivorans*. *Appl. Environ. Microbiol.* *84*, e01185-18. <https://doi.org/10.1128/AEM.01185-18>.
42. Thompson, M.G., Incha, M.R., Pearson, A.N., Schmidt, M., Sharpless, W.A., Eiben, C.B., Cruz-Morales, P., Blake-Hedges, J.M., Liu, Y., Adams, C.A., et al. (2020). Fatty acid and alcohol metabolism in *Pseudomonas putida*: functional analysis using random barcode transposon sequencing. *Appl. Environ. Microbiol.* *86*, e01665-20. <https://doi.org/10.1128/AEM.01665-20>.
43. Jahn, M., Crang, N., Janasch, M., Hober, A., Forsström, B., Kimler, K., Mattausch, A., Chen, Q., Asplund-Samuelsson, J., and Hudson, E.P. (2021). Protein allocation and utilization in the versatile chemolithoautotroph *Cupriavidus necator*. *Elife* *10*, e69019. <https://doi.org/10.7554/eLife.69019>.
44. Morin, M., Pierce, E.C., and Dutton, R.J. (2018). Changes in the genetic requirements for microbial interactions with increasing community complexity. *Elife* *7*, e37072. <https://doi.org/10.7554/eLife.37072>.
45. Pierce, E.C., Morin, M., Little, J.C., Liu, R.B., Tannous, J., Keller, N.P., Pogliano, K., Wolfe, B.E., Sanchez, L.M., and Dutton, R.J. (2021). Bacterial-fungal interactions revealed by genome-wide analysis of bacterial mutant fitness. *Nat. Microbiol.* *6*, 87–102. <https://doi.org/10.1038/s41564-020-00800-z>.
46. Borchert, A.J., Bleem, A., and Beckham, G.T. (2022). Experimental and analytical approaches for improving the resolution of randomly barcoded transposon insertion sequencing (RB-TnSeq) studies. *ACS Synth. Biol.* *11*, 2015–2021. <https://doi.org/10.1021/acssynbio.2c00119>.
47. Stothard, P., Grant, J.R., and Van Domselaar, G. (2019). Visualizing and comparing circular genomes using the CGView family of tools. *Brief. Bioinform.* *20*, 1576–1582. <https://doi.org/10.1093/bib/bbx081>.
48. Abe, T., Masai, E., Miyauchi, K., Katayama, Y., and Fukuda, M. (2005). A tetrahydrofolate-dependent O-demethylase, LigM, is crucial for catabolism of vanillate and syringate in *Sphingomonas paucimobilis* SYK-6. *J. Bacteriol.* *187*, 2030–2037. <https://doi.org/10.1128/JB.187.6.2030-2037.2005>.
49. Kasai, D., Kamimura, N., Tani, K., Umeda, S., Abe, T., Fukuda, M., and Masai, E. (2012). Characterization of FerC, a MarR-type transcriptional regulator, involved in transcriptional regulation of the ferulate catabolic operon in *Sphingobium* sp. strain SYK-6. *FEMS Microbiol. Lett.* *332*, 68–75. <https://doi.org/10.1111/j.1574-6968.2012.02576.x>.
50. Kamimura, N., and Masai, E. (2014). The protocatechuate 4,5-cleavage pathway: overview and new findings. In *Biodegradative Bacteria*, H. Nojiri, M. Tsuda, M. Fukuda, and Y. Kamagata, eds. (Springer Japan), pp. 207–226. [https://doi.org/10.1007/978-4-431-54520-0\\_10](https://doi.org/10.1007/978-4-431-54520-0_10).
51. Hogancamp, T.N., and Raushel, F.M. (2018). Functional annotation of LigU as a 1,3-allylic isomerase during the degradation of lignin in the protocatechuate 4,5-cleavage pathway from the soil bacterium *Sphingobium* sp. SYK-6. *Biochemistry* *57*, 2837–2845. <https://doi.org/10.1021/acs.biochem.8b00295>.
52. Kamimura, N., Takamura, K., Hara, H., Kasai, D., Natsume, R., Senda, T., Katayama, Y., Fukuda, M., and Masai, E. (2010). Regulatory system of the protocatechuate 4,5-cleavage pathway genes essential for lignin downstream catabolism. *J. Bacteriol.* *192*, 3394–3405. <https://doi.org/10.1128/JB.00215-10>.
53. Masai, E., Momose, K., Hara, H., Nishikawa, S., Katayama, Y., and Fukuda, M. (2000). Genetic and biochemical characterization of 4-carboxy-2-hydroxyruconate-6-semialdehyde dehydrogenase and its role in the protocatechuate 4,5-cleavage pathway in *Sphingomonas paucimobilis* SYK-6. *J. Bacteriol.* *182*, 6651–6658. <https://doi.org/10.1128/JB.182.23.6651-6658.2000>.

54. Hara, H., Masai, E., Miyauchi, K., Katayama, Y., and Fukuda, M. (2003). Characterization of the 4-carboxy-4-hydroxy-2-oxoadipate aldolase gene and operon structure of the protocatechuate 4,5-cleavage pathway genes in *Sphingomonas paucimobilis* SYK-6. *J. Bacteriol.* *185*, 41–50. <https://doi.org/10.1128/JB.185.1.41-50.2003>.
55. Kasai, D., Masai, E., Katayama, Y., and Fukuda, M. (2007). Degradation of 3-O-methylgallate in *Sphingomonas paucimobilis* SYK-6 by pathways involving protocatechuate 4,5-dioxygenase. *FEMS Microbiol. Lett.* *274*, 323–328. <https://doi.org/10.1111/j.1574-6968.2007.00855.x>.
56. Araki, T., Umeda, S., Kamimura, N., Kasai, D., Kumano, S., Abe, T., Kawazu, C., Otsuka, Y., Nakamura, M., Katayama, Y., et al. (2019). Regulation of vanillate and syringate catabolism by a MarR-type transcriptional regulator DesR in *Sphingobium* sp. SYK-6. *Sci. Rep.* *9*, 18036. <https://doi.org/10.1038/s41598-019-54490-7>.
57. Mori, K., Niinuma, K., Fujita, M., Kamimura, N., and Masai, E. (2018). DdvK, a novel major facilitator superfamily transporter essential for 5,5'-dehydrodivanillate uptake by *Sphingobium* sp. strain SYK-6. *Appl. Environ. Microbiol.* *84*, e01314–18. <https://doi.org/10.1128/AEM.01314-18>.
58. Fujita, M., Mori, K., Hara, H., Hishiyama, S., Kamimura, N., and Masai, E. (2019). A TonB-dependent receptor constitutes the outer membrane transport system for a lignin-derived aromatic compound. *Commun. Biol.* *2*, 432. <https://doi.org/10.1038/s42003-019-0676-z>.
59. Kuatsjah, E., Chen, H.-M., Withers, S.G., and Eltis, L.D. (2017). Characterization of an extradiol dioxygenase involved in the catabolism of lignin-derived biphenyl. *FEBS Lett.* *591*, 1001–1009. <https://doi.org/10.1002/1873-3468.12611>.
60. Kuatsjah, E., Chan, A.C.K., Kobylarz, M.J., Murphy, M.E.P., and Eltis, L.D. (2017). The bacterial meta-cleavage hydrolase LigY belongs to the amidohydrolase superfamily, not to the  $\alpha/\beta$ -hydrolase superfamily. *J. Biol. Chem.* *292*, 18290–18302. <https://doi.org/10.1074/jbc.M117.797696>.
61. Peng, X., Masai, E., Kasai, D., Miyauchi, K., Katayama, Y., and Fukuda, M. (2005). A second 5-carboxyvanillate decarboxylase gene, *ligW2*, is important for lignin-related biphenyl catabolism in *Sphingomonas paucimobilis* SYK-6. *Appl. Environ. Microbiol.* *71*, 5014–5021. <https://doi.org/10.1128/AEM.71.9.5014-5021.2005>.
62. Palamuru, S., Dellas, N., Pearce, S.L., Warden, A.C., Oakeshott, J.G., and Pandey, G. (2015). Phylogenetic and kinetic characterization of a suite of dehydrogenases from a newly isolated bacterium, strain SG61-1L, that catalyze the turnover of guaiacylglycerol- $\beta$ -guaiacyl ether stereoisomers. *Appl. Environ. Microbiol.* *81*, 8164–8176. <https://doi.org/10.1128/AEM.01573-15>.
63. Higuchi, Y., Aoki, S., Takenami, H., Kamimura, N., Takahashi, K., Hishiyama, S., Lancefield, C.S., Ojo, O.S., Katayama, Y., Westwood, N.J., and Masai, E. (2018). Bacterial catabolism of  $\beta$ -hydroxypropiovanillone and  $\beta$ -hydroxypropiosyringone produced in the reductive cleavage of arylglycerol- $\beta$ -aryl ether in lignin. *Appl. Environ. Microbiol.* *84*, e02670–17. <https://doi.org/10.1128/AEM.02670-17>.
64. Zakzeski, J., Bruijninx, P.C.A., Jongerius, A.L., and Weckhuysen, B.M. (2010). The catalytic valorization of lignin for the production of renewable chemicals. *Chem. Rev.* *110*, 3552–3599. <https://doi.org/10.1021/cr900354u>.
65. Subbotina, E., Rukkijakan, T., Marquez-Medina, M.D., Yu, X., Johnsson, M., and Samec, J.S.M. (2021). Oxidative cleavage of C–C bonds in lignin. *Nat. Chem.* *13*, 1118–1125. <https://doi.org/10.1038/s41557-021-00783-2>.
66. Dao Thi, H., Van Aelst, K., Van den Bosch, S., Katahira, R., Beckham, G.T., Sels, B.F., and Van Geem, K.M. (2022). Identification and quantification of lignin monomers and oligomers from reductive catalytic fractionation of pine wood with GC  $\times$  GC – FID/MS. *Green Chem.* *24*, 191–206. <https://doi.org/10.1039/D1GC03822B>.
67. Presley, G.N., Werner, A.Z., Katahira, R., Garcia, D.C., Haugen, S.J., Ramirez, K.J., Giannone, R.J., Beckham, G.T., and Michener, J.K. (2021). Pathway discovery and engineering for cleavage of a  $\beta$ -1 lignin-derived biaryl compound. *Metab. Eng.* *65*, 1–10. <https://doi.org/10.1016/j.ymben.2021.02.003>.
68. Kuatsjah, E., Zahn, M., Chen, X., Kato, R., Hinchey, D.J., Konev, M.O., Katahira, R., Orr, C., Wagner, A., Zou, Y., et al. (2023). Biochemical and structural characterization of a Sphingomonad diarylpropane retro-aldolase for cofactorless deformylation. *Proc. Natl. Acad. Sci. USA* *120*, e2212246120. <https://doi.org/10.1073/pnas.2212246120>.
69. Kishi, K., Habu, N., Samejima, M., and Yoshimoto, T. (1991). Purification and some properties of the enzyme catalyzing the C $\gamma$ -elimination of a diarylpropane-type lignin model from *Pseudomonas paucimobilis* TMY1009. *Agric. Biol. Chem.* *55*, 1319–1323. <https://doi.org/10.1080/00021369.1991.10870761>.
70. Kuatsjah, E., Chan, A.C.K., Katahira, R., Haugen, S.J., Beckham, G.T., Murphy, M.E.P., and Eltis, L.D. (2021). Structural and functional analysis of lignostilbene dioxygenases from *Sphingobium* sp. SYK-6. *J. Biol. Chem.* *296*, 100758. <https://doi.org/10.1016/j.jbc.2021.100758>.
71. Masai, E., Sasaki, M., Minakawa, Y., Abe, T., Sonoki, T., Miyauchi, K., Katayama, Y., and Fukuda, M. (2004). A novel tetrahydrofolate-dependent O-demethylase gene is essential for growth of *Sphingomonas paucimobilis* SYK-6 with syringate. *J. Bacteriol.* *186*, 2757–2765. <https://doi.org/10.1128/JB.186.9.2757-2765.2004>.
72. Fujita, M., Sakumoto, T., Tanatani, K., Yu, H., Mori, K., Kamimura, N., and Masai, E. (2020). Iron acquisition system of *Sphingobium* sp. strain SYK-6, a degrader of lignin-derived aromatic compounds. *Sci. Rep.* *10*, 12177. <https://doi.org/10.1038/s41598-020-68984-2>.
73. Varman, A.M., He, L., Follenfant, R., Wu, W., Wemmer, S., Wrobel, S.A., Tang, Y.J., and Singh, S. (2016). Decoding how a soil bacterium extracts building blocks and metabolic energy from ligninolysis provides road map for lignin valorization. *Proc. Natl. Acad. Sci. USA* *113*, E5802–E5811. <https://doi.org/10.1073/pnas.1606043113>.
74. Fernández-Sandoval, M.T., Huerta-Beristain, G., Trujillo-Martinez, B., Bustos, P., González, V., Bolivar, F., Gosset, G., and Martínez, A. (2012). Laboratory metabolic evolution improves acetate tolerance and growth on acetate of ethanologenic *Escherichia coli* under non-aerated conditions in glucose-mineral medium. *Appl. Microbiol. Biotechnol.* *96*, 1291–1300. <https://doi.org/10.1007/s00253-012-4177-y>.
75. Karp, E.M., Donohoe, B.S., O'Brien, M.H., Ciesielski, P.N., Mittal, A., Bidy, M.J., and Beckham, G.T. (2014). Alkaline pretreatment of corn stover: bench-scale fractionation and stream characterization. *ACS Sus. Chem. Eng.* *2*, 1481–1491. <https://doi.org/10.1021/sc500126u>.
76. Vardon, D.R., Franden, M.A., Johnson, C.W., Karp, E.M., Guarneri, M.T., Linger, J.G., Salm, M.J., Strathmann, T.J., and Beckham, G.T. (2015). Adipic acid production from lignin. *Energy Environ. Sci.* *8*, 617–628. <https://doi.org/10.1039/C4EE03230F>.
77. Karp, E.M., Nimlos, C.T., Deutch, S., Salvachúa, D., Cywar, R.M., and Beckham, G.T. (2016). Quantification of acidic compounds in complex biomass-derived streams. *Green Chem.* *18*, 4750–4760. <https://doi.org/10.1039/C6GC00868B>.
78. Karlen, S.D., Fasahati, P., Mazaheri, M., Serate, J., Smith, R.A., Sirobushanam, S., Chen, M., Tymokhin, V.I., Cass, C.L., Liu, S., et al. (2020). Assessing the viability of recovery of hydroxycinnamic acids from lignocellulosic biorefinery alkaline pretreatment waste streams. *ChemSusChem* *13*, 2012–2024. <https://doi.org/10.1002/cssc.201903345>.
79. Saboe, P.O., Tomashek, E.G., Monroe, H.R., Haugen, S.J., Prestangen, R.L., Cleveland, N.S., Happs, R.M., Miscall, J., Ramirez, K.J., Katahira, R., et al. (2022). Recovery of low molecular weight compounds from alkaline pretreatment liquor via membrane separations. *Green Chem.* *24*, 3152–3166. <https://doi.org/10.1039/D2GC00075J>.
80. Gibson, R.P., Tarling, C.A., Roberts, S., Withers, S.G., and Davies, G.J. (2004). The donor subsite of trehalose-6-phosphate synthase. *J. Biol. Chem.* *279*, 1950–1955. <https://doi.org/10.1074/jbc.M307643200>.
81. Miao, Y., Tenor, J.L., Toffaletti, D.L., Maskarinec, S.A., Liu, J., Lee, R.E., Perfect, J.R., and Brennan, R.G. (2017). Structural and *in vivo* studies on trehalose-6-phosphate synthase from pathogenic fungi provide insights into its catalytic mechanism, biological necessity, and potential for novel

- antifungal drug design. *mBio* 8, e00643–17. <https://doi.org/10.1128/mBio.00643-17>.
82. Styrvoid, O.B., and Strøm, A.R. (1991). Synthesis, accumulation, and excretion of trehalose in osmotically stressed *Escherichia coli* K-12 strains: influence of amber suppressors and function of the periplasmic trehalase. *J. Bacteriol.* 173, 1187–1192. <https://doi.org/10.1128/jb.173.3.1187-1192.1991>.
  83. Belda, E., van Heck, R.G.A., José Lopez-Sanchez, M., Cruveiller, S., Barbe, V., Fraser, C., Klenk, H.-P., Petersen, J., Morgat, A., Nikel, P.I., et al. (2016). The revisited genome of *Pseudomonas putida* KT2440 enlightens its value as a robust metabolic chassis: Re-annotation of the *Pseudomonas putida* KT2440 genome. *Environ. Microbiol.* 18, 3403–3424. <https://doi.org/10.1111/1462-2920.13230>.
  84. Maia, L.B., Moura, J.J.G., and Moura, I. (2015). Molybdenum and tungsten-dependent formate dehydrogenases. *J. Biol. Inorg. Chem.* 20, 287–309. <https://doi.org/10.1007/s00775-014-1218-2>.
  85. Traxler, M.F., Summers, S.M., Nguyen, H.-T., Zacharia, V.M., Hightower, G.A., Smith, J.T., and Conway, T. (2008). The global, ppGpp-mediated stringent response to amino acid starvation in *Escherichia coli*. *Mol. Microbiol.* 68, 1128–1148. <https://doi.org/10.1111/j.1365-2958.2008.06229.x>.
  86. Nelson, K.E., Weinel, C., Paulsen, I.T., Dodson, R.J., Hilbert, H., Martins dos Santos, V.A.P., Fouts, D.E., Gill, S.R., Pop, M., Holmes, M., et al. (2002). Complete genome sequence and comparative analysis of the metabolically versatile *Pseudomonas putida* KT2440. *Environ. Microbiol.* 4, 799–808. <https://doi.org/10.1046/j.1462-2920.2002.00366.x>.
  87. Jungnickel, K.E.J., Parker, J.L., and Newstead, S. (2018). Structural basis for amino acid transport by the CAT family of SLC7 transporters. *Nat. Commun.* 9, 550. <https://doi.org/10.1038/s41467-018-03066-6>.
  88. Nikel, P.I., Chavarria, M., Fuhrer, T., Sauer, U., and de Lorenzo, V. (2015). *Pseudomonas putida* KT2440 strain metabolizes glucose through a cycle formed by enzymes of the Entner-Doudoroff, Embden-Meyerhof-Parnas, and pentose phosphate pathways. *J. Biol. Chem.* 290, 25920–25932. <https://doi.org/10.1074/jbc.M115.687749>.
  89. Fenster, J.A., and Eckert, C.A. (2021). High-throughput functional genomics for energy production. *Curr. Opin. Biotechnol.* 67, 7–14. <https://doi.org/10.1016/j.copbio.2020.09.010>.
  90. Kamimura, N., Goto, T., Takahashi, K., Kasai, D., Otsuka, Y., Nakamura, M., Katayama, Y., Fukuda, M., and Masai, E. (2017). A bacterial aromatic aldehyde dehydrogenase critical for the efficient catabolism of syringaldehyde. *Sci. Rep.* 7, 44422. <https://doi.org/10.1038/srep44422>.
  91. Benjamini, Y., and Hochberg, Y. (1995). Controlling the false discovery rate: a practical and powerful approach to multiple testing. *J. Roy. Stat. Soc. B Met.* 57, 289–300. <https://doi.org/10.1111/j.2517-6161.1995.tb02031.x>.
  92. Storey, J.D., and Tibshirani, R. (2003). Statistical significance for genome-wide studies. *Proc. Natl. Acad. Sci. USA* 100, 9440–9445. <https://doi.org/10.1073/pnas.1530509100>.
  93. Choi, K.-H., Kumar, A., and Schweizer, H.P. (2006). A 10-min method for preparation of highly electrocompetent *Pseudomonas aeruginosa* cells: application for DNA fragment transfer between chromosomes and plasmid transformation. *J. Microbiol. Methods* 64, 391–397. <https://doi.org/10.1016/j.mimet.2005.06.001>.
  94. Johnson, C.W., and Beckham, G.T. (2015). Aromatic catabolic pathway selection for optimal production of pyruvate and lactate from lignin. *Metab. Eng.* 28, 240–247. <https://doi.org/10.1016/j.ymben.2015.01.005>.

## STAR★METHODS

### KEY RESOURCES TABLE

REAGENT or RESOURCE	SOURCE	IDENTIFIER
<b>Bacterial strains</b>		
Bacterial strains, see <a href="#">Table S9</a>	This study	N/A
<b>Chemicals and recombinant proteins</b>		
Kanamycin monosulfate	GoldBio	K-120-5; CAS: 25389-94-0
2,6-diaminopimelic acid	ACROS Organics	AC235540010; CAS: 583-93-7
DpnI enzyme	New England Biolabs	R0176
Q5 HiFi 2X Master Mix	New England Biolabs	M0492
Ferulic acid	Sigma-Aldrich	128708; CAS: 537-98-4
Vanillin	Sigma-Aldrich	V1104; CAS: 121-33-5
Vanillic acid	Sigma-Aldrich	94770; CAS: 121-34-6
4-hydroxybenzoic acid	Sigma-Aldrich	240141; CAS: 99-96-7
Syringaldehyde	Sigma-Aldrich	S7602; CAS: 134-96-3
Methanol	Sigma-Aldrich	34860; CAS: 67-56-1
Acetic acid (sodium salt)	Sigma-Aldrich	S2889; CAS: 127-09-3
Protocatechuic acid	ACROS Organics	AC114890250; CAS: 99-50-3
Syringic acid	AK Scientific	C591; CAS: 530-57-4
DDVA	Oakwood Chemical	375175; CAS: 2134-90-9
GGE	TCI America	G0233; CAS: 7382-59-4
Trehalose	Research Products International	T82000; CAS: 6138-23-4
L-Methionine	Sigma-Aldrich	M9625; CAS: 63-68-3
β-1 dimer compounds	This study	CHEBI:86530
<b>Critical commercial assays</b>		
GeneJet Genomic DNA Purification Kit	Thermo Scientific	K0721
Monarch Genomic DNA Purification Kit	New England Biolabs	T3010S
Quantifluor dsDNA Sample Kit	Promega	E2671
NucleoSpin PCR Clean-Up Kit	Macherey-Nagel	740609
Zymoclean Gel DNA Recovery Kit	Zymo Research	D4007
DNA1000 Kit	Agilent	5067-1505
NEBNext Ultra II FS DNA Library Prep Kit with NEBNext Sample Purification Beads	New England Biolabs	E6177S
<b>Deposited data</b>		
Raw sequencing reads	This study	SRA: PRJNA905394
<b>Oligonucleotides</b>		
Oligonucleotides, see <a href="#">Table S9</a>	This study	N/A
<b>Recombinant DNA</b>		
Plasmids, see <a href="#">Table S9</a>	This study	N/A
<b>Software and algorithms</b>		
RB-TnSeq analysis scripts	Wetmore et al. <sup>38</sup>	<a href="https://bitbucket.org/berkeleylab/feba/src/master/">https://bitbucket.org/berkeleylab/feba/src/master/</a>
Custom python scripts for fitness comparisons	This study	<a href="https://github.com/beckham-lab/SYK-6_RB-TnSeq">https://github.com/beckham-lab/SYK-6_RB-TnSeq</a> , <a href="https://doi.org/10.5281/zenodo.8066380">https://doi.org/10.5281/zenodo.8066380</a>

## RESOURCE AVAILABILITY

### Lead contact

Further information and requests for resources and reagents should be directed to and will be fulfilled by the lead contact, Gregg Beckham ([gregg.beckham@nrel.gov](mailto:gregg.beckham@nrel.gov)).

### Materials availability

The plasmids and strains listed in the Supplementary Information are available upon request, via a Materials Transfer Agreement with the National Renewable Energy Laboratory.

### Data and code availability

All sequencing data (fastq files) were deposited at the NCBI Sequence Read Archive (SRA) with accession number PRJNA905394 and are publicly available as of the date of publication. Analysis of RB-TnSeq and BarSeq data was performed using a combination of previously described<sup>38</sup> scripts (<https://bitbucket.org/berkeleylab/feba/src/master/>) and custom Python scripts ([https://github.com/beckham-lab/SYK-6\\_RB-TnSeq](https://github.com/beckham-lab/SYK-6_RB-TnSeq), <https://doi.org/10.5281/zenodo.8066380>). Gene fitness data for each experiment are reported in Table S3. Any additional information required to reanalyze the data reported in the paper is available from the lead contact upon request.

## EXPERIMENTAL MODEL AND SUBJECT DETAILS

All bacterial plasmids, DNA oligos, and strains designed and used in this study are listed in Table S9. Growth conditions for individual bacteria strains could be found in the method details section and Table S10.

## METHOD DETAILS

### Generation of a randomly barcoded Tn5 transposon mutant library in SYK-6

The Tn5 transposon mutant library was generated by conjugating SYK-6 with *E. coli* WM3064 harboring the pKMW7 barcoded Tn5 transposon vector library (APA766; see Table S9). A single colony of SYK-6 was used to inoculate a culture in lysogeny broth (LB; 10 g/L Bacto tryptone, 5 g/L yeast extract, and 5 g/L NaCl), which was then grown overnight at 30°C and 225 rpm. A frozen aliquot of APA766 was cultivated overnight at 37°C and 225 rpm in LB + 50 µg/mL kanamycin (Km50) + 60 µg/mL 2,6-diaminopimelic acid (DAP). The APA766 culture was washed twice with sterile PBS and resuspended in LB medium. The optical density at 600 nm (OD<sub>600nm</sub>) of the APA766 suspension and the SYK-6 overnight culture were measured, and four aliquots of cells were mixed at a 1:1 ratio (500 µL each). Mixtures were centrifuged at 8000 g for 3 min and resuspended in 100 µL LB medium. 40 µL of each mixture was plated in duplicate on 0.45-µm nitrocellulose filters overlaid on LB + 60 µg/mL DAP agar plates (8 total conjugations). Plates were incubated for 12 h at room temperature, and then cells were transferred from the filters into LB medium and plated onto LB + Km50 (24 plates) to select for transconjugants. Plates were incubated at 30°C for 3 days, and then all colonies were scraped from the plates and pooled into LB + Km50 liquid medium. The pooled mixture was diluted 1:3 in LB + Km50 and grown at 30°C and 225 rpm in a baffled flask for 6 h. Four 1 mL aliquots of cells were pelleted at 8,000 g for 1 min, and gDNA was collected from each using the Thermo GeneJet Genomic DNA Purification Kit according to manufacturer instructions. Frozen aliquots of the remaining library culture were combined with 10% glycerol and stored at –80°C for future use.

### Preparation of the transposon mutant library for sequencing

Two gDNA preparations from the SYK-6 transposon mutant library were quantified with the Promega QuantiFluor dsDNA Sample Kit. The NEBNext Ultra II FS DNA Library Prep Kit (New England Biolabs) was used to perform enzymatic fragmentation (200–450 bp size), end repair, and A-tailing with 500 ng of each gDNA preparation according to the manufacturer recommendations. Previously described Illumina Y adapters (Mod2\_TS\_Univ and Mod2\_Truseq)<sup>38</sup> were annealed to each other by combining 5 µL of each 100 µM oligonucleotide in a PCR tube and incubating with the following program: 30 min at 37°C; ramp up 0.5°C per s to 97.5°C; hold at 97.5°C for 155 s; ramp down 0.1°C per 5 s for 775 cycles; hold at 4°C. Adapters were diluted to 15 µM in TE buffer and stored at –80°C until use. The annealed Y adapters were ligated onto gDNA templates using the NEBNext kit according to manufacturer instructions. Adapter-ligated DNA was cleaned up with NEBNext Sample Purification Beads (New England Biolabs) according to the protocol for 320–470 bp DNA. Purified DNA was eluted from the beads with 0.1X TE. The eluted DNA was used as a template in PCR reactions to amplify only the bar-coded regions with the Nspacer\_barseq\_universal primer (specific to transposon) and the P7\_MOD\_TS\_index primer (specific to Y-adapter).<sup>38</sup> Each reaction was a 100 µL volume and utilized 500 nM of each primer. Thermal cycles were as follows: (i) 94°C–2 min, (ii) 25 cycles of: 94°C–30 s; 65°C–20 s; 72°C–30 s, (iii) 72°C–10 min. After PCR, 1 µL of DpnI enzyme (New England Biolabs) was added to each reaction and tubes were incubated at 37°C for 1 h. The products were cleaned up with the NucleoSpin PCR Clean-Up Kit (Macherey-Nagel) according to manufacturer instructions. The two parent library preparations were pooled and the size and concentration of the sample were determined on a Bioanalyzer with the DNA1000 Kit (Agilent). The sample was paired-end sequenced (2 x 150 bp) on an Illumina HiSeq instrument (GENEWIZ).

### TnSeq data analysis

TnSeq reads were analyzed according to a previously established workflow using published perl scripts.<sup>38</sup> First, MapTnSeq.pl was run with default parameters to identify barcodes within the gDNA sequencing reads. Next, barcodes that consistently mapped to a unique location in the genome were identified with DesignRandomPool.pl (Table S1). Barcodes were required to map uniquely to their primary location at least 10 times.

### Competitive mutant fitness assays

Conditions for fitness assays were based on those used in prior work,<sup>25,33,34,36,57,73,90</sup> which demonstrated growth on most of the compounds in this study as sole sources of carbon and energy. For conditions that had not been previously studied, growth curves are included in the results section. Unless otherwise listed, competitive fitness assays with the SYK-6 transposon insertion library were carried out in Wx medium.<sup>49</sup> For fitness profiling with aromatic monomer compounds, acetate stress, DDVA, and GGE, three aliquots of the library were thawed on ice and inoculated into 25 mL LB medium or Wx-SEMP medium (Wx with 10 mM sucrose, 10 mM glutamate, 130  $\mu$ M L-Met, and 10 mM proline) in 125 mL baffled flasks. These “baseline” (time zero) cultures were grown at 30°C and 225 rpm until the OD<sub>600nm</sub> of each reached ~1.0, at which point 2 x 1 mL of cells were centrifuged at 10,000 g for 1 min and frozen at –80°C. The remainder of each baseline culture was centrifuged at 3,000 g for 3 min and then resuspended in 5 mL Wx medium. The washed baseline cultures were inoculated to an initial OD<sub>600nm</sub> of 0.04 in flasks containing Wx medium with carbon sources defined in Table S10. The “enrichment” cultures were grown at 30°C and 225 rpm until late log phase (OD<sub>600nm</sub> values at collection time varied depending on condition; see Table S10), at which point 2 x 1 mL of cells were centrifuged at 10,000 g for 1 min and frozen at –80°C. SYK-6 is auxotrophic for L-Met in the absence of compounds with an O-methyl group,<sup>72</sup> so L-Met was supplemented to these conditions (*p*-coumarate, 4-hydroxybenzoate, and protocatechuate) to support growth. In the case of GGE, growth was quite slow, so cultures were inoculated to an initial OD<sub>600nm</sub> of 0.1 for this condition (Wx + 1 mM GGE) and its corresponding control (Wx + 1 mM vanillate). For fitness profiling with L-Met stress and  $\beta$ -1 dimer compounds, a single aliquot of the SYK-6 transposon insertion library was thawed on ice and inoculated into 50 mL LB medium in a 250 mL baffled flask. This “baseline” (time zero) culture was grown at 30°C and 225 rpm for 16 h, at which point 2 x 1 mL of cells were centrifuged at 10,000 g for 1 min and frozen at –80°C. The remainder of the baseline culture was centrifuged at 3,000 g for 3 min and then resuspended in 5 mL Wx medium. The washed baseline culture was inoculated (technical triplicates) to an initial OD<sub>600nm</sub> of 0.05 in microtiter plates containing 150  $\mu$ L Wx medium with carbon sources defined in Table S10. Plates were incubated at maximum shaking speed and 30°C in a BioscreenC instrument (Growth Curves Ltd.), and optical density measurements were taken every 15 min with a wideband (400–600 nm) filter. When cultures reached late log phase (cell density values at collection time varied depending on condition; see Table S10), the full volume of all three wells per condition was collected in a single tube and centrifuged at 10,000 g for 1 min and frozen at –80°C.

### Preparation of samples for BarSeq

gDNA was extracted from each cell pellet from the competitive mutant fitness assays using either the Thermo GeneJet Genomic DNA Purification Kit or the Monarch Genomic DNA Purification Kit (New England Biolabs) according to manufacturer instructions. 75 ng of each gDNA sample was used as template for a 15  $\mu$ L PCR reaction, including 7.5  $\mu$ L Q5 High-Fidelity 2X Master Mix (New England Biolabs), 1.5  $\mu$ L 5  $\mu$ M BarSeq\_P1 primer (common reverse primer; previously described<sup>38</sup>), 1.5  $\mu$ L 5  $\mu$ M BarSeq\_P2 primer (a uniquely indexed forward primer, IT001-IT044; previously described<sup>38</sup>), 1  $\mu$ L 30% v/v DMSO, and nuclease-free water. Thermal cycles were performed as follows: (i) 98°C–4 min, (ii) 25 cycles of: 98°C–30 s; 55°C–30 s; 72°C–30 s, (iii) 72°C–5 min. 4  $\mu$ L of each PCR product was run on a 1% agarose gel to ensure all samples amplified. 8  $\mu$ L of each PCR product was then combined in a single 1.5 mL tube to make the sequencing pool, and 5  $\mu$ L of DpnI enzyme was added to digest template gDNA. The entire pool was run and excised from a 1% agarose gel, and DNA was purified with the Zymoclean Gel DNA Recovery Kit (Zymo Research). Columns were eluted with nuclease-free water, and the pool was analyzed for purity and concentration on a Qubit instrument (Thermo Fisher). Paired-end sequencing (2 x 150 bp) of the BarSeq pool was performed on an Illumina HiSeq instrument (GENEWIZ).

### Fitness analysis

Sequencing reads were initially analyzed with a series of previously described perl scripts.<sup>38</sup> MultiCodes.pl identified the barcode in each read of a demultiplexed fastq file and made a table of how often each barcode was seen; combineBarSeq.pl merged the table of counts from MultiCodes.pl with the parent pool file from DesignRandomPool.pl to make a table of how often each strain was seen. Next, BarSeqR.pl was run with the ‘-noR’ option to generate a table of barcode counts for all fitness conditions. All samples passed quality control metrics as defined by the perl scripts, except for one of the replicates in the LB baseline condition that lacked sufficient reads, so fitness comparisons were calculated relative to the two LB baseline samples instead of all three. Next, strain and gene fitness calculations were performed as previously described,<sup>38</sup> but with a custom Python script translated from the original FEBA.R code ([https://github.com/beckham-lab/SYK-6\\_RB-TnSeq](https://github.com/beckham-lab/SYK-6_RB-TnSeq)). Gene fitness values were calculated only for genes in the SYK-6 genome and not for those on the pSLG plasmid. This analysis did not trim transposon insertion counts from the ends of the gene and normalization was applied only as for small gene scaffolds.<sup>38</sup> For statistical analysis of gene fitness significance in samples with a single replicate, the previously described t-like test statistic was used.<sup>38</sup> For analysis of samples in triplicate, comparison of mean fitness

values between two enrichment conditions was facilitated by a two-sample *t* test ([https://github.com/beckham-lab/SYK-6\\_RB-TnSeq](https://github.com/beckham-lab/SYK-6_RB-TnSeq)), using adjusted *p* values (*q* values) to correct for multiple testing by the False Discovery Rate (FDR) method.<sup>91,92</sup> Normalized gene fitness scores and *t*-like test statistics for all replicates and conditions may be found in Table S3.

### Bacterial strains, plasmids, and culture conditions

The plasmids, primers, and strains designed and used in this study are described in Table S9. Construction details for engineered strains are also listed in Table S9. For generation of engineered mutants of *P. putida*, cells were prepared for electroporation according to a previously described method,<sup>93</sup> and then they were transformed with 500 ng of pK18sB-based plasmids or 200 ng of each helper (pGW31) and cargo (pE5k-based) plasmid. Colonies were selected on LB + Km50 agar. For pK18sB-based integration, antibiotic selection was performed twice and sucrose counter-selection was performed twice according to a previously established protocol.<sup>94</sup> Unless otherwise noted, strains were cultivated in LB medium. SYK-6,  $\Delta$ 07730,  $\Delta$ 07740,  $\Delta$ 02610, and  $\Delta$ 02610(pSEVA02610) were grown at 30°C and 160 rpm for 24 h cultures. *E. coli* strains were grown at 37°C and 160 rpm. *P. putida* and its mutants were grown at 30°C and 225 rpm. PCR reactions for cloning utilized Q5 High-Fidelity 2X Master Mix (New England Biolabs) and genes of interest were cloned by Gibson assembly using the NEBuilder HiFi DNA Assembly Master Mix (New England Biolabs).

### Growth assays for SYK-6 and engineered mutants thereof

For L-Met tolerance assays on agar, cells of SYK-6,  $\Delta$ 02610, and  $\Delta$ 02610(pSEVA02610) were cultured in liquid LB medium for 24 h. The cells were harvested by centrifugation at 14,000 *g* for 1 min at 4°C and washed twice with 5 mL of Wx buffer (12.5 mM KH<sub>2</sub>PO<sub>4</sub>, 27.4 mM Na<sub>2</sub>HPO<sub>4</sub>, 7.6 mM (NH<sub>4</sub>)<sub>2</sub>SO<sub>4</sub>, pH 7.1), and then suspended in Wx buffer to an OD<sub>600nm</sub> of 1.0. 5-fold serial dilutions were prepared with the same buffer and 7  $\mu$ L of each cell solution were dropped onto agar plates containing Wx medium with 5 mM vanillate or 5 mM 4-hydroxybenzoate and 0–100  $\mu$ M L-Met and incubated for 5 days at 30°C. For assessment of acetate tolerance, biological triplicate cultures of SYK-6 were inoculated from single colonies into 5 mL of LB medium and grown overnight at 225 rpm and 30°C. Media was prepared by mixing appropriate volumes of 2X Wx-SEMP medium, 500 mM acetate (pH 7.0), and sterile water to achieve a range of acetate concentrations in Wx-SEMP. 2  $\mu$ L of each overnight culture was inoculated directly into one of three wells in a microtiter plate containing 200  $\mu$ L of media. Plates were incubated at maximum shaking speed and 30°C in a BioscreenC Pro instrument (Growth Curves Ltd.), and optical density measurements were taken every 15 min at 600 nm. A similar protocol was used for assessment of growth with DDVA, where triplicate overnight cultures of SYK-6,  $\Delta$ 07730, and  $\Delta$ 07740 were passaged from LB into a microtiter plate filled with Wx medium +5 mM DDVA. Growth was measured every 3 h with continuous shaking.

### Growth assays for *P. putida* and engineered mutants thereof

For assessment of acetate tolerance in *P. putida*, biological triplicate cultures of KT2440 wild-type, ACB283, and ACB285 were inoculated from single colonies into 5 mL of LB medium and grown overnight at 225 rpm and 30°C. Media was prepared by mixing appropriate volumes of 2X M9 medium, 500 mM acetate (pH 7.0), 2.78 M glucose, and sterile water to achieve 1X M9 medium (6.78 g/L Na<sub>2</sub>HPO<sub>4</sub>, 3 g/L KH<sub>2</sub>PO<sub>4</sub>, 0.5 g/L NaCl, 1 g/L NH<sub>4</sub>Cl, 2 mM MgSO<sub>4</sub>, 100  $\mu$ M CaCl<sub>2</sub>, and 18  $\mu$ M FeSO<sub>4</sub>) with 20 mM glucose and a range of acetate concentrations. 2  $\mu$ L of each overnight culture was inoculated directly into one of three wells in a microtiter plate containing 200  $\mu$ L of media. Plates were incubated at maximum shaking speed and 30°C in a BioscreenC Pro instrument (Growth Curves Ltd.), and optical density measurements were taken every 15 min at 600 nm. Growth rates were calculated as the slope of the natural logarithm of OD<sub>600nm</sub> as a function of time during exponential phase, and lag times were calculated as the time required to reach half the maximum cell density (OD<sub>600nm</sub>).

### Compound preparation and sourcing

The  $\beta$ -1 dimer compounds *threo*-DGPD, *erythro*-DGPD, *threo*-DHPD, and *erythro*-DHPD were synthesized, purified, and analyzed in-house according to previously established protocols.<sup>67</sup> Please refer to Presley et al.<sup>67</sup> for detailed synthesis methods and compound verification. Lignostilbene was a gift from the laboratory of Lindsay Eltis. Components of media (M9, Wx, and LB) were from Sigma-Aldrich. Ferulic acid, vanillin, vanillic acid, 4-hydroxybenzoic acid, syringaldehyde, methanol, L-Met, and acetic acid were also from Sigma-Aldrich. Protocatechuic acid and 2,6-diaminopimelic acid were from ACROS Organics, syringic acid was from AK Scientific, DDVA was from Oakwood Chemical, GGE was from TCI America, and trehalose was from Research Products International. TCI America confirmed the presence of the four GGE stereoisomers by NMR, and a majority of isomers took the *erythro* form ((*R,S*) or (*S,R*)).

## QUANTIFICATION AND STATISTICAL ANALYSIS

Detailed descriptions and code for statistical analysis of gene fitness is described in the “fitness analysis” section of the [method details](#). Briefly, evaluation of the *t*-like test statistic for individual gene fitness was carried out as previously described by Wetmore et al.,<sup>38</sup> and comparison of two mean fitness values utilized a two-sample *t* test with *q* values to correct for multiple testing.<sup>91,92</sup> The null hypothesis of the two-sample *t* test assumed that the mean fitness values of the two groups were the same. For growth assays in Figures 5, 6, and 7, error bars indicate the standard deviation from the mean of three biological replicates.